Beam Dynamics with Space Charge in IOTA

Runze Li, University of Wisconsin Madison

David Feigelson, University of Chicago, SIST Intern Summer 2021

Tanaji Sen and Jean-Francois Ostiguy, Fermilab

This research was enabled by the Fermilab 2020 Lee Teng Internship Program

Motivation

1. The original motivation is a possible experiment to explore echo formation in the the presence of space charge forces.

2. Validation and development of pyORBIT code as a simulation tool to support the IOTA program

3. Model the IOTA proton beam with space charge effects in:
    1. purely linear lattice
    2. lattice with octupole insert
    3. lattice with nonlinear lens (Danilov-Nagaitsev)

4. Explore the role of space charge driven coherent and incoherent resonances in emittance growth and particle loss. Investigate quasi-integrability and complete integrability in mitigating these resonances

5. Excite a coherent quadrupole mode; deduce the incoherent space charge tune spread and emittance.

6. Observe how the initial transverse distribution affects coherent tune shift and beam quality

Outline

- Tests without space charge
  - Dynamic aperture test
  - Tune footprint test
- Tests with space charge using longitudinal bunched beam
  - Bunch preparation
  - Slow initialization procedure
  - 0 amplitude tune shift and tune footprint
  - Emittance change and particle loss with octupole insert
- Tests with space charge using longitudinal coasting beam
  - Bunch preparation
  - 0 amplitude tune shift and tune footprint
  - Initial particle loss against theory with realistic aperture
  - Emittance change and particle loss with realistic aperture and octupole insert
- Emittance growth (simulation vs theory) and RMS matching
- Benchmarking pyORBIT with ImpactZ
- Part of this presentation is based on the report FERMILAB-TM-2753-AD available at https://arxiv.org/abs/2106.03327

Part I: Tests without Space Charge

4

IOTA Proton Beam Parameters

- Simulation injection point is the middle of octupole insert region, where $\beta_x = \beta_y = \beta$ and $D_x = D_y = \alpha_x = \alpha_y = 0$. RMS matching at this high symmetry location reduces the number of fit parameters.
- Nonlinear elements have been removed as well as nonlinear body and edge corrections in dipoles and quadrupoles.
- Physical apertures are set at 0.1 m to prevent particle loss

$$\beta_x = \beta_y$$

$$0 = \alpha_x = \alpha_y = D_x = D'_x$$

beam size $\sigma_x = \sigma_y \sim 1.63$mm

Initial start of lattice

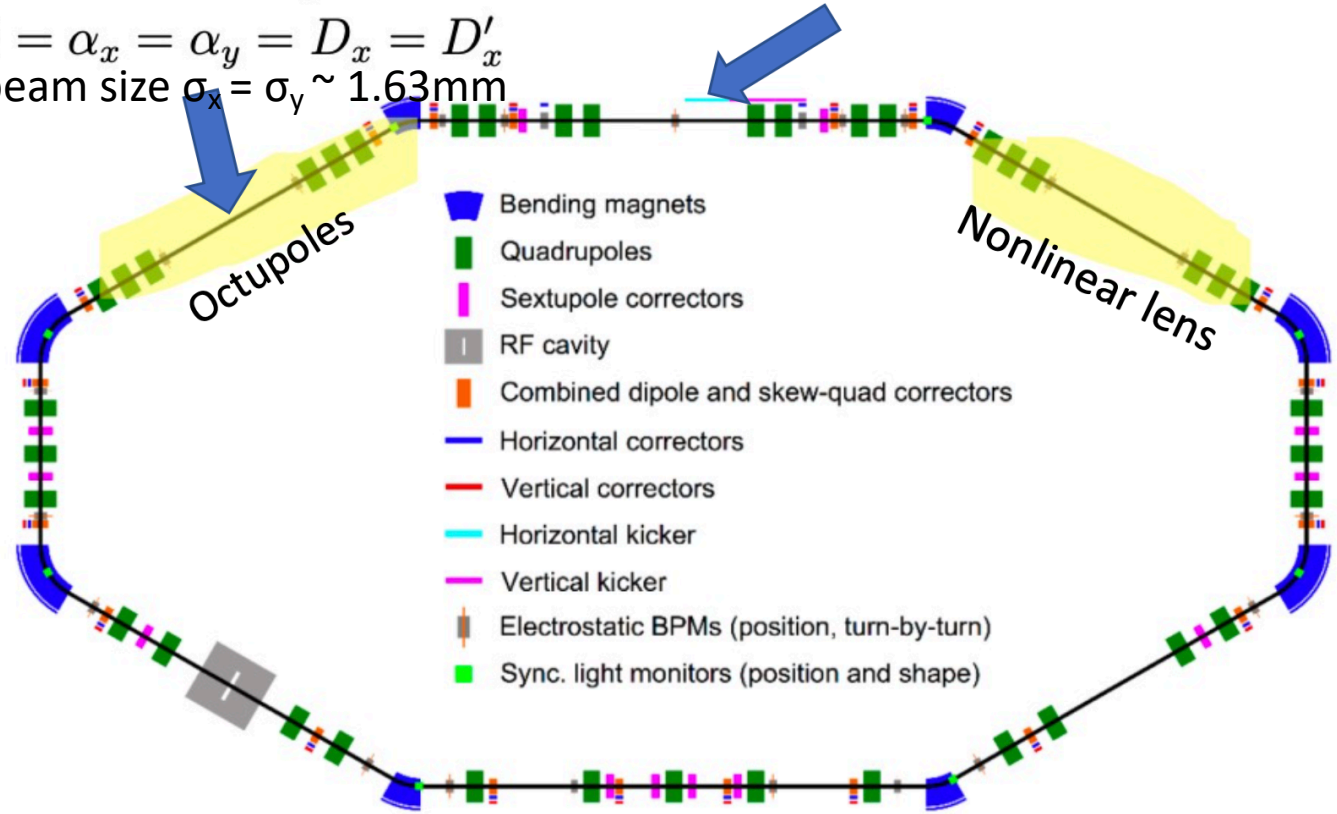

IOTA proton parameters	
Circumference	39.97 [m]
Kinetic Energy	2.5 [MeV]
Maximum bunch intensity /current	9×10^{10} / 8 [mA]
Transverse normalized rms emittance	(0.3, 0.3) [mm-mrad]
Betatron tunes	(5.3, 5.3)
Natural chromaticities	(-8.2, -8.1)
Average transverse beam sizes (rms)	(2.22, 2.22) [mm]
Kinematic γ / Transition γ_T	1.003 / 3.75
Rf voltage	400 [V]
Rf frequency / harmonic number	2.2 [MHz] / 4
Bucket wavelength	$\sim$ 10 [m]
Bucket half height in $\Delta p/p$	3.72×10^{-3}
rms bunch length	1.7 [m]
rms energy /momentum spread	1.05×10^{-5} / 1.99×10^{-3}
Beam pipe radius	25 [mm]
Bunch density	6.9×10^{14} [m^{-3}]
Plasma period τ_p	0.18 [μ-sec] / 0.1 [turns]
Average Debye length λ_D	559 [μm]

Dynamic Aperture of IOTA Lattice with Octupole Insert

- This test aims to compare the dynamic apertures of the IOTA lattice with octupoles obtained with pyORBIT and MADX
- With physical aperture set at 25mm, 5000 test particles (50 amplitudes, 100 angles between 0 and 90 deg.) are initialized as:
    1. 4D: RF Cavity is turned off, particles are initialized at (x_i, 0, y_i, 0, 0, 0)
    2. 5D: RF Cavity is turned off, particles are initialized (x_i, 0, y_i, 0, 0, σ_p) Chromaticity effect included
    3. 6D: RF Cavity is turned on, particles are initialized (x_i, 0, y_i, 0, 0, σ_p), so synchrotron motion is included
- After tracking for 10000 turns, the largest excursions of the surviving particles yield an upper bound for the dynamic aperture
- Results from MADX and pyORBIT are in **excellent agreement**

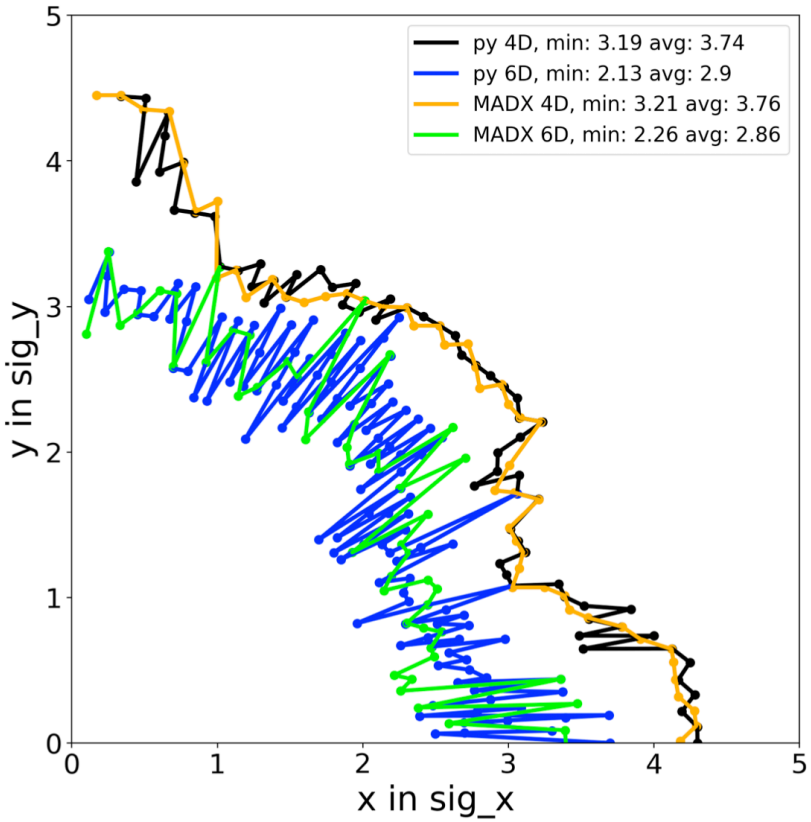

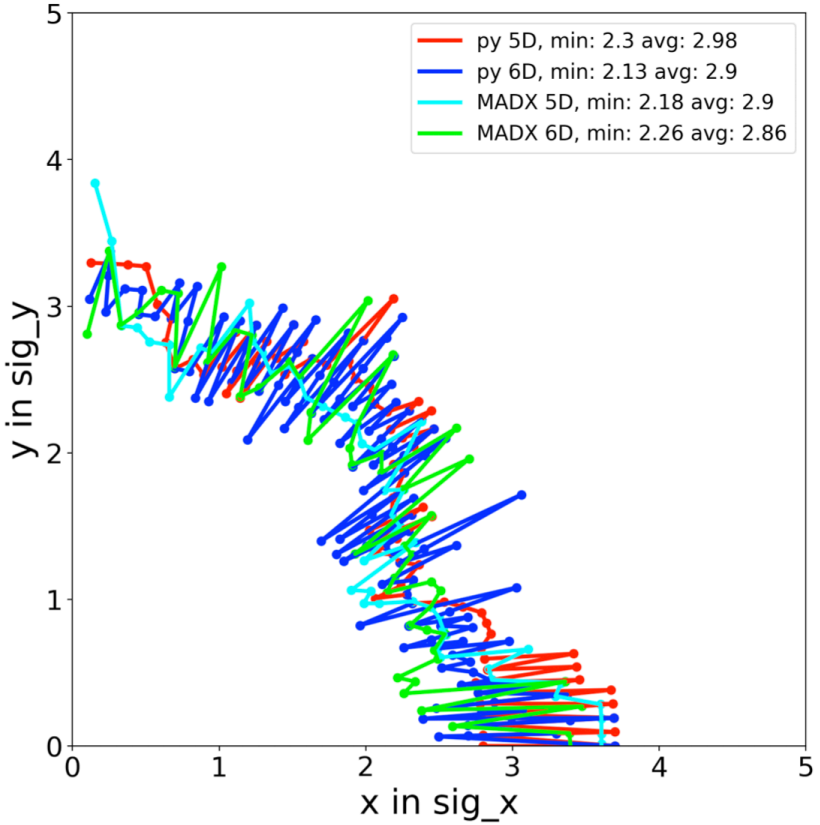

Aperture type	Minimum DA		Average DA	
	pyORBIT	MADX	pyORBIT	MADX
4D	3.19	3.21	3.74	3.76
5D	2.3	2.18	2.98	2.9
6 D	2.13	2.26	2.9	2.86

4D, 5D (left) and 6D (right) dynamic apertures and their minimum and average values from MADX and pyORBIT

6

Tune Footprint of IOTA Lattice with Octupole Insert

- This test aims to compare the tune footprints obtained with pyORBIT and MADX in the presence of an octupole insert .
- Test particles are initialized uniformly in the x-y planes from (0, 0, 0, 0, 0, 0) to ($5\sigma_x$, 0, $5\sigma_y$, 0, 0, 0) and tracked for 5000 turns in both pyORBIT and MADX using the IOTA lattice with octupoles as the only source of nonlinearity.
- For all the survivors, x and y are recorded at each turn and an FFT is used to extract the tunes Q_x and Q_y (left plot):

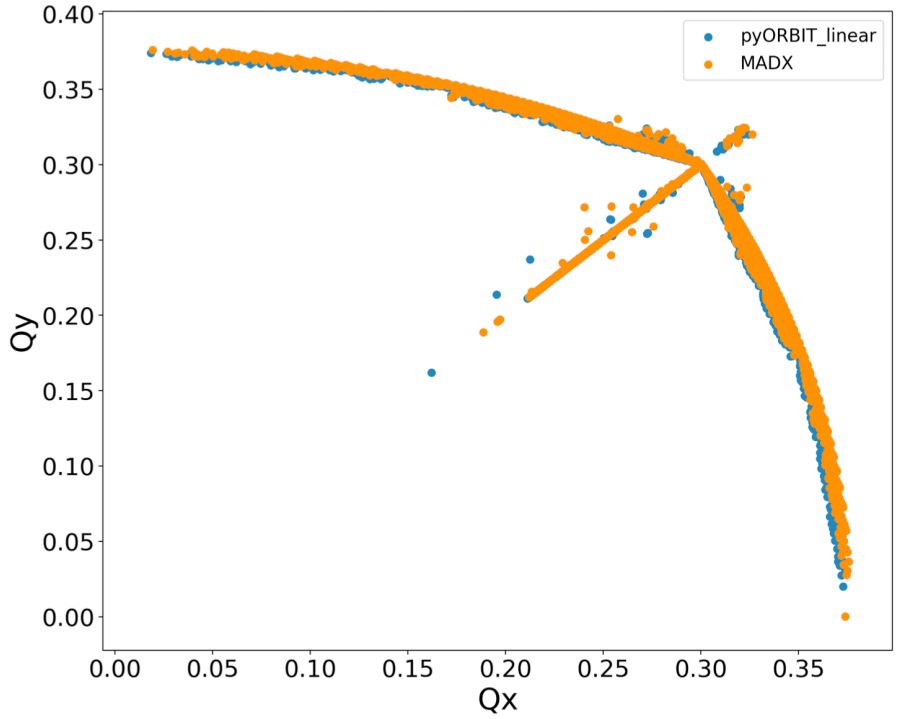

Tune footprint of IOTA with octupoles calculated from MADX and pyORBIT

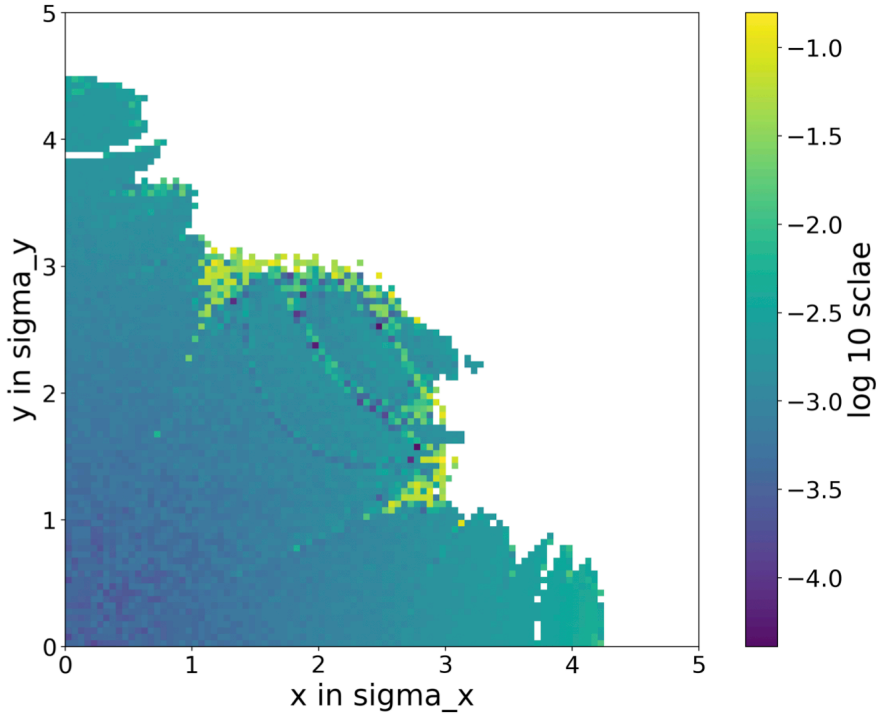

Difference in tune calculated by MADX and pyORBIT for test particles at different initial positions

- The right plot shows the absolute difference in tunes $dQ = |Q_{x,P} - Q_{x,M}| + |Q_{y,P} - Q_{y,M}|$ calculated by MADX and pyORBIT for test particles initialized at different positions. The tune variation map is similar to the one obtained with FMA. While FMA uses the same code to evaluate tune differences, here, two are used.

Part II: Space charge with a bunched beam

8

Space Charge Simulation in pyORBIT

- pyORBIT uses a particle-in-cell (PIC) model to simulate space charge effect. Macro particles representing the charged particles in a bunch and are deposited on a grid; a smoothed density is extracted by interpolation. The electric potential is found by numerically solving Poisson's equation in the beam rest frame using a standard FFT based algorithm.
- The simulation assumes an open boundary and **no longitudinal space charge effect**
- Gaussian initial distributions with unnormalized emittances 4.11um are used in planes x-px and y-py
- A waterbag distribution is used in the longitudinal plane. Particles are uniformly distributed within an inner Hamiltonian contour inside the separatrix defined by the RF to prevent particles leaking out of the bucket.
- In pyORBIT, the accuracy of the space charge solver is mainly determined by the number of macroparticles (MP), the number of space charge kicks per betatron wavelength (Nsc), and the number of spatial grid points (Nx × Ny × Nz). After some systemic convergence tests shown in the backup slides, #MPs = 5e5, grid size 128x128x5, and Nsc = 63 are used in all following tests. This choice is optimized to ensure a converged solution while keeping computation time reasonable.

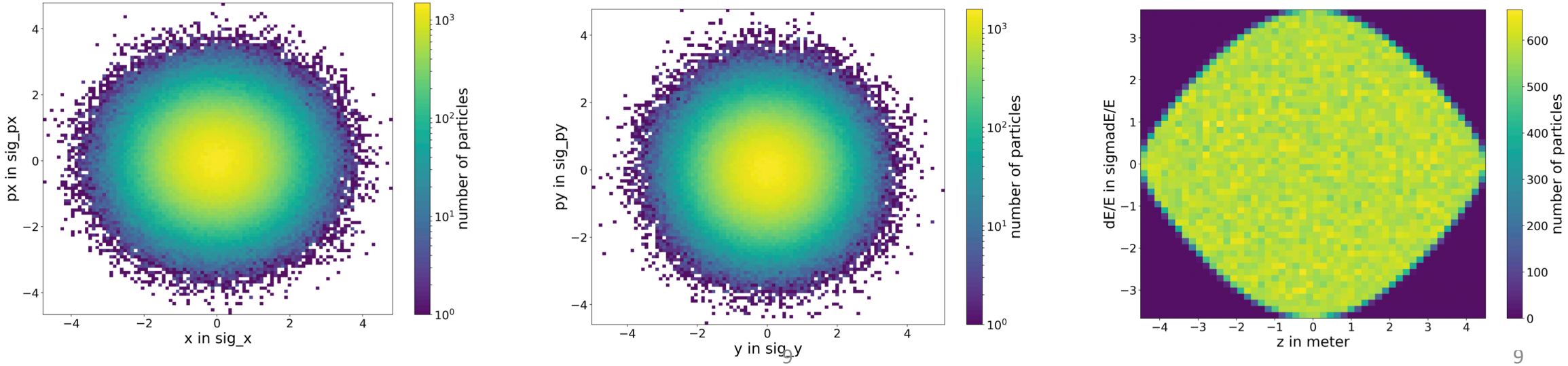

Particle distribution in x-px, y-py, and z-dE plane

9

Slow Initialization Procedure

- At full intensity, without any specific initial matching procedure and a limiting aperture radius of 100 mm, the emittance grows 10-fold and 1% of the particles are lost after 1000 turns.

- Slow initialization is a procedure to establish a steady state. Rather than injecting with the full charge, the charge per macroparticle is increased linearly from zero to its full value at turn T_{init}, the initialization time. Provided this process is sufficiently adiabatic, one expects the beam to remain in near equilibrium at every step as the beam has time to adjust to a slowly changing space charge force.

- In order to find the optimal T_{init}, the bunch is tracked for totally 500 turns including different T_{init} turns for initialization. The percentage particle loss and relative emittance growth are shown

- The default T_{init} is set to be 40 turns; this corresponds to the smallest particle loss.

- In the range considered for T_{init} , relative emittance growth is 15% while particle losses varies ~ 40 fold.

- Since in all cases the rms emittance keeps growing, the core does not reach the aperture, so all loss comes from the halo. It seems that the transverse tails of the beam reacts to intensity changes on a faster time scale than the core

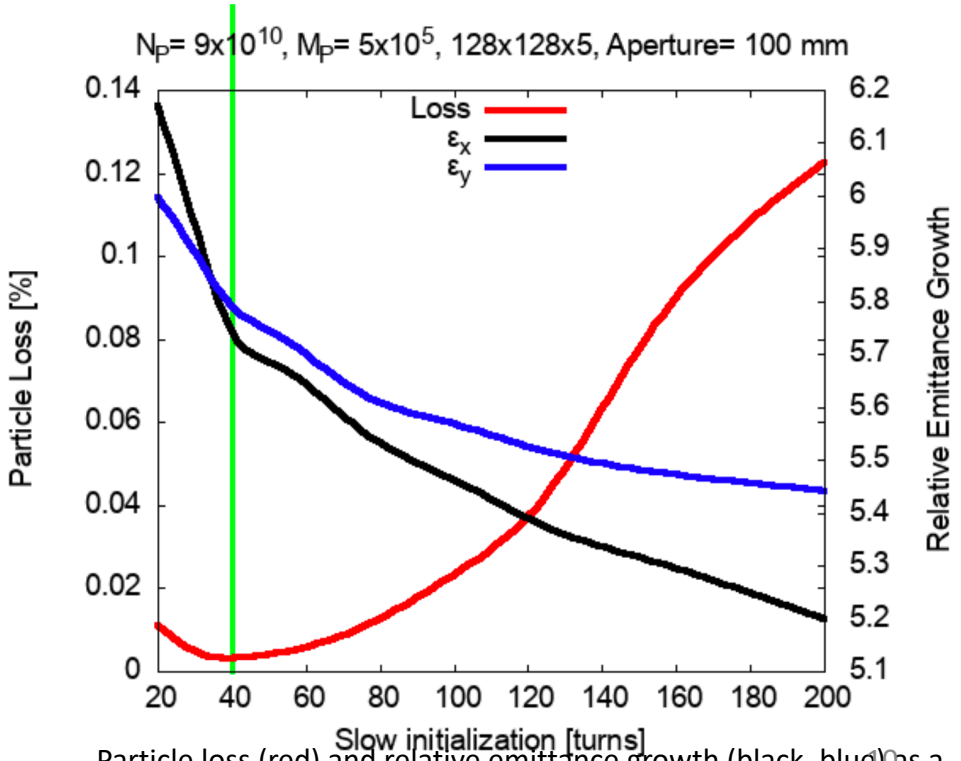

Particle loss (red) and relative emittance growth (black, blue) as a function of different number of initialization turns

Zero-Amplitude Tune Shift in the Presence of Space Charge

- For a bunch with transverse gaussian distribution, the analytical zero-amplitude tune shift is:

$$\Delta Q_{0,sc} = \frac{r_p}{\beta_k \gamma^2 \varepsilon_N} \bar{\lambda}_L N_p R$$

where r_p is the classical proton radius, β and γ are Lorentz factors, R is effective machine radius, ε_N is normalized transverse emittance, N_p is the number of protons per bunch, and $\bar{\lambda}_L$ is the effective line density

- For our bunch setup, it is:

$$\Delta Q_{0,sc} = \frac{-1.09 * 10^{-17} * N_p}{\langle \varepsilon_N \rangle}$$

where $< \varepsilon_N >$ is the time averaged normalized transverse emittance. Rapid initial increase of the emittance reduces the space charge tune shifts from nominal values.

- The transverse tune shift is not very sensitive to the specifics of the longitudinal distribution, as shown in the following plot

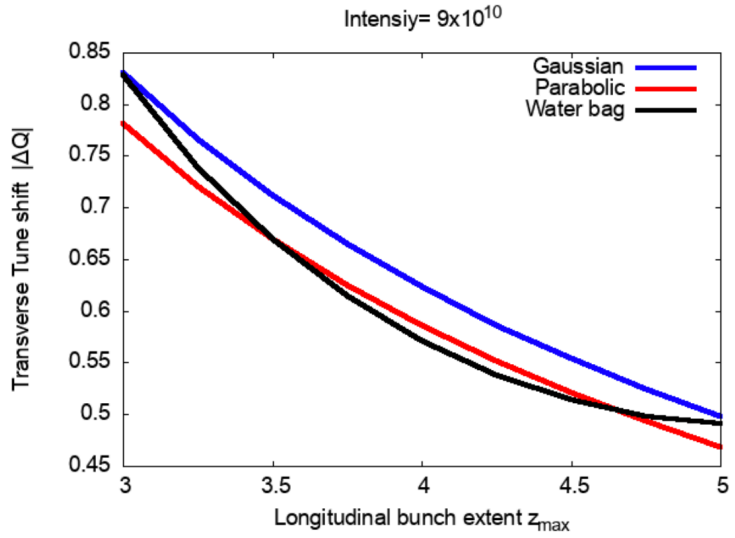

Absolute transverse tune shift as a function of the longitudinal extent Z_{max} for different distributions

Zero-Amplitude Tune Shift in the Presence of Space Charge

- Once the bunch has stabilized, test particles are added at ($\sqrt{n^2\beta_x\epsilon_x}cos\theta$, $-\sqrt{\frac{n^2\epsilon_x}{\beta_x}}(cos\theta + \alpha_x sin\theta)$, 0, 0, 0, 0), where n 0.01 < n < 8 and 0 < θ < 2pi. Tunes are calculated from betatron oscillations over 100 turns.
- The process is repeated for 2 intensities: full intensity (Q=9e10) and a lower intensity (Q=1e10)

	Normalized ϵ_x when stable	dQx at 0 amplitude
Full Intensity	1.31 mm-mrad	-0.747
Lower Intensity	0.360 mm-mrad	-0.303

Test particle distribution

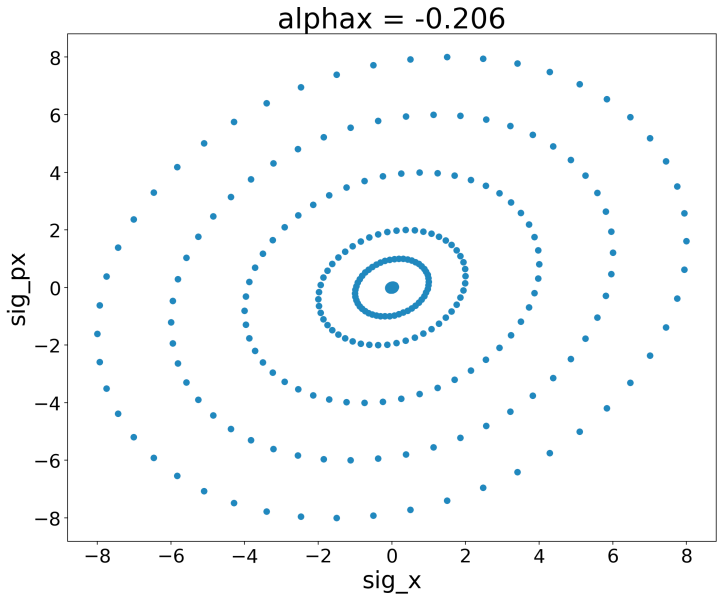

Tune Distribution at Full Intensity

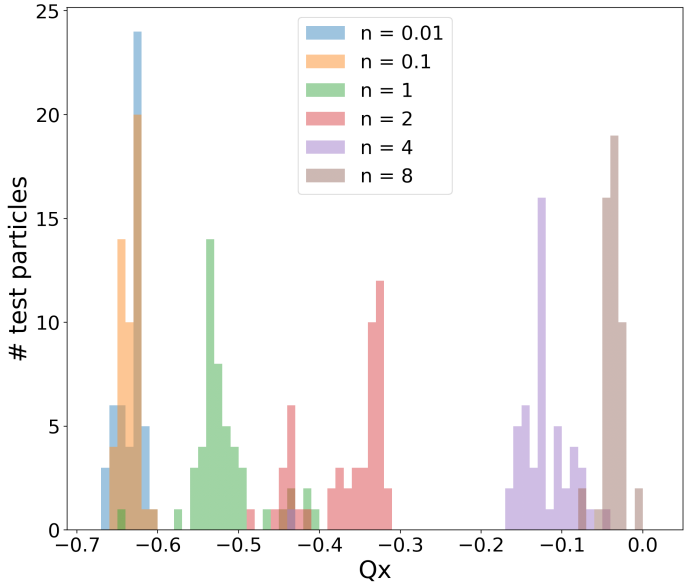

Tune Distribution at Lower Intensity

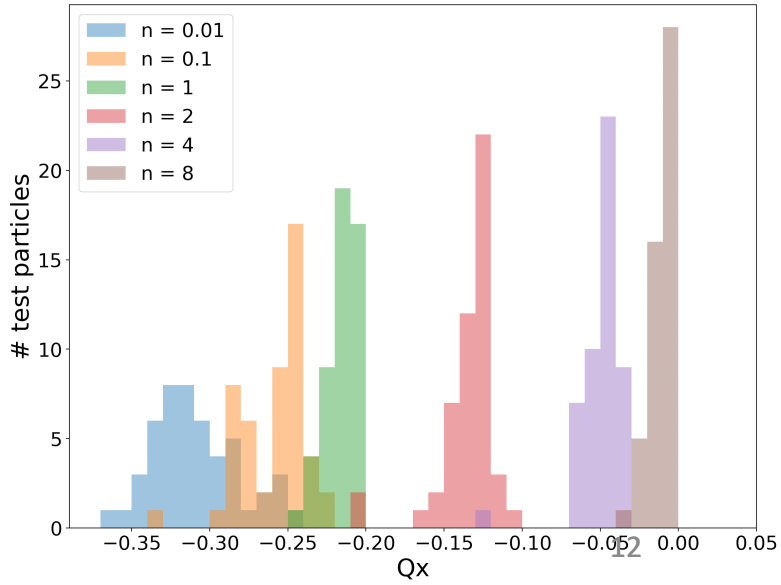

Tune Footprint

At full intensity (Q=9e10), after slow initialization and stabilization, test particles are injected with initial positions on semi-circular arcs of radius (0 - 8)σ in *x*–*y* space. The test particles are tracked for 100 turns and tunes are extracted by counting zero-crossings.

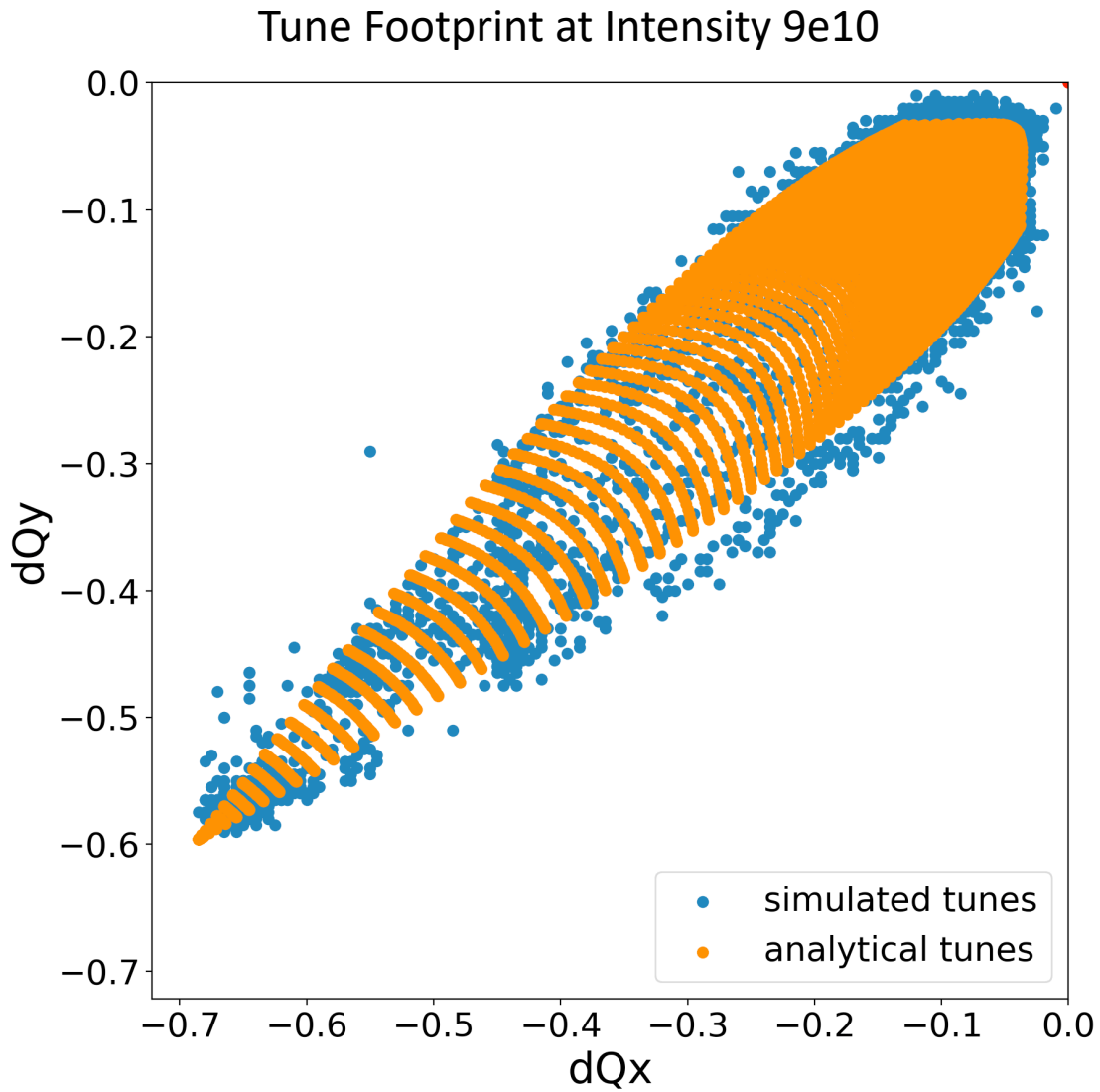

Emittance evolution and particle loss with octupole insert, large aperture, and transverse gaussian

- At intensities 1e9 and 1e10, full and half octupole strengths, and 0.1m aperture, the bunch is tracked for 1000 turns
- At ½ octupole strength, the emittance at both intensities does not stabilize after 1000 turns.
- At full octupole strength, the bunch quickly reach the dynamic aperture boundary.
  Particle loss is >5% at intensity 1e9 and >20% for 1e10
- Dispersion increases horizontal beam size and reduces horizontal space charge forces. The result is less horizontal emittance growth.

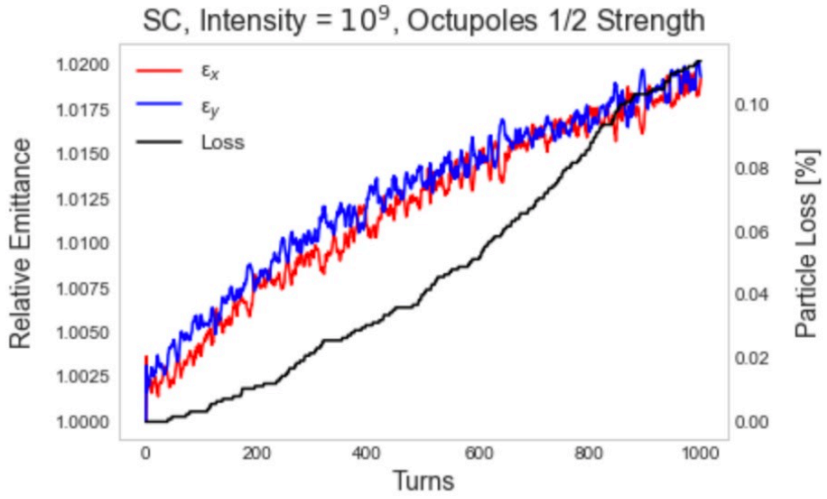

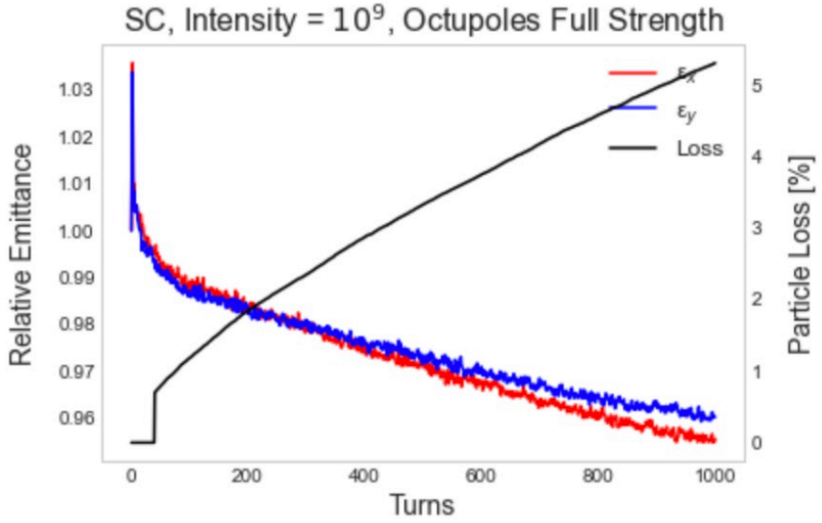

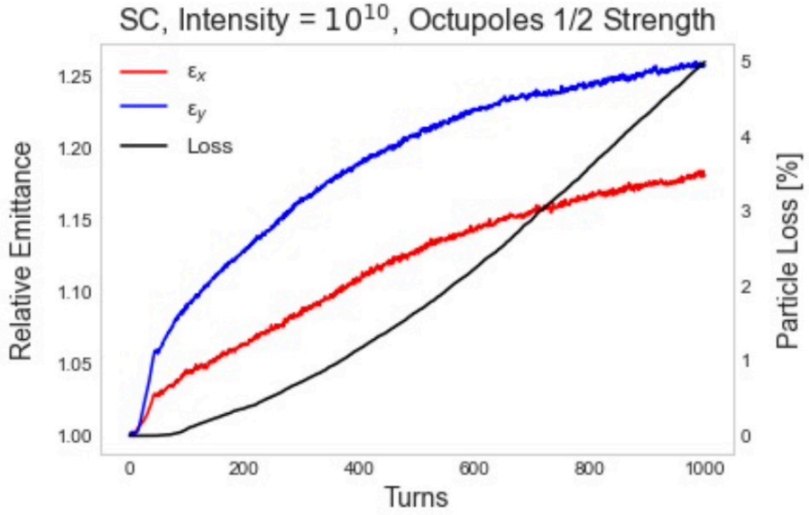

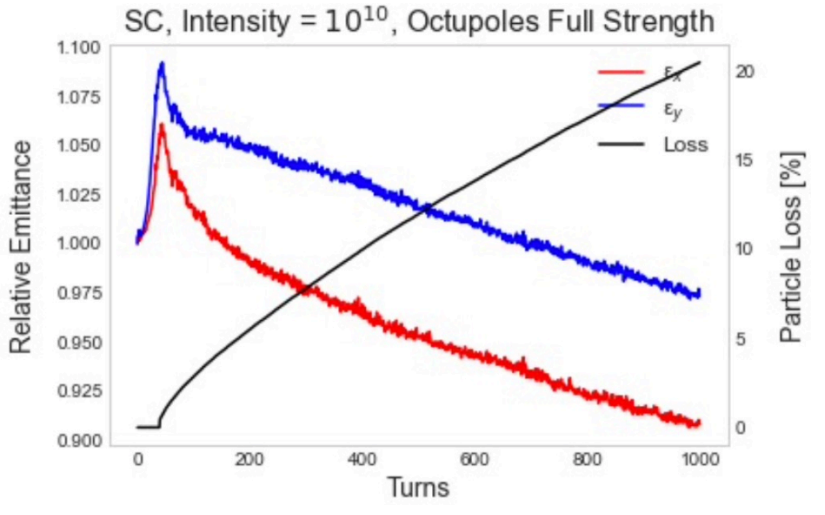

Emittance change and particle loss with octupole insert, large aperture, and transverse truncated gaussian

- For intensity 1e10 and 9e10, gaussian distribution truncated at 1.5σ is used
- For intensity 1e10, the bunch core does not hit DA in 1000 turns. At Octupole ½ strength, loss ~1%; at Octupole full strength, loss ~ 8%
- For intensity 9e10, particles hit DA even at half strength, loss skyrockets to ~70%/80% . Emittance grows 2-4 times

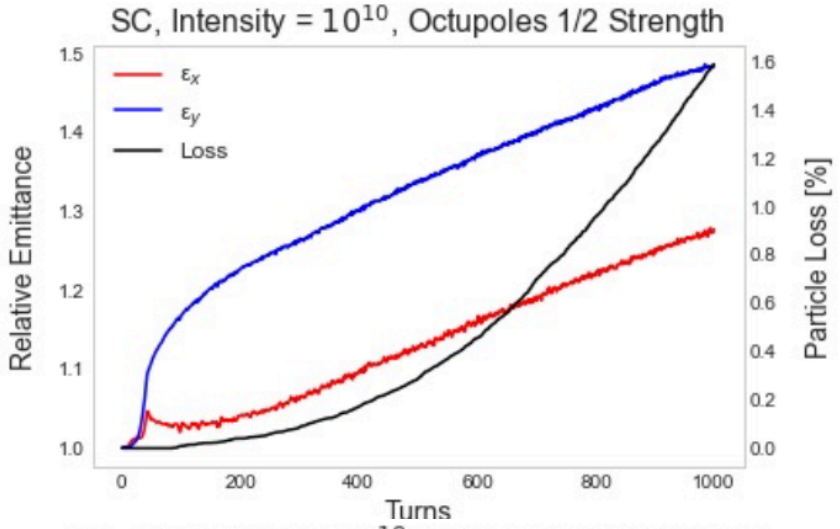

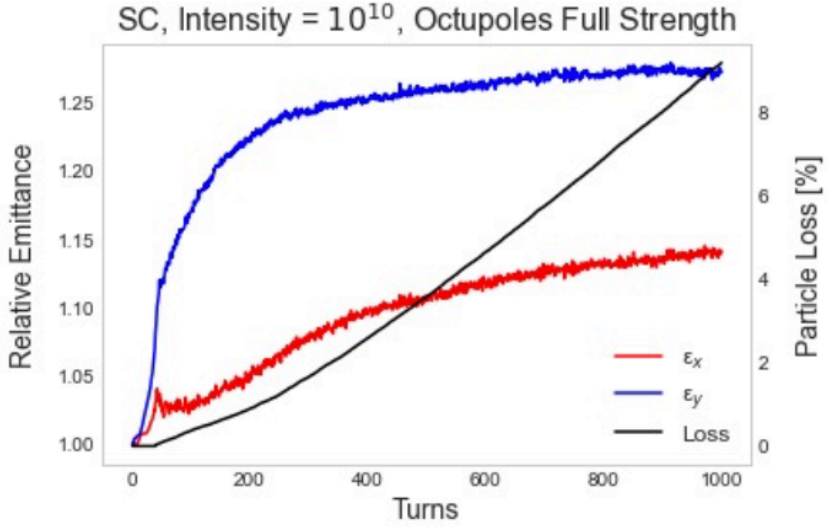

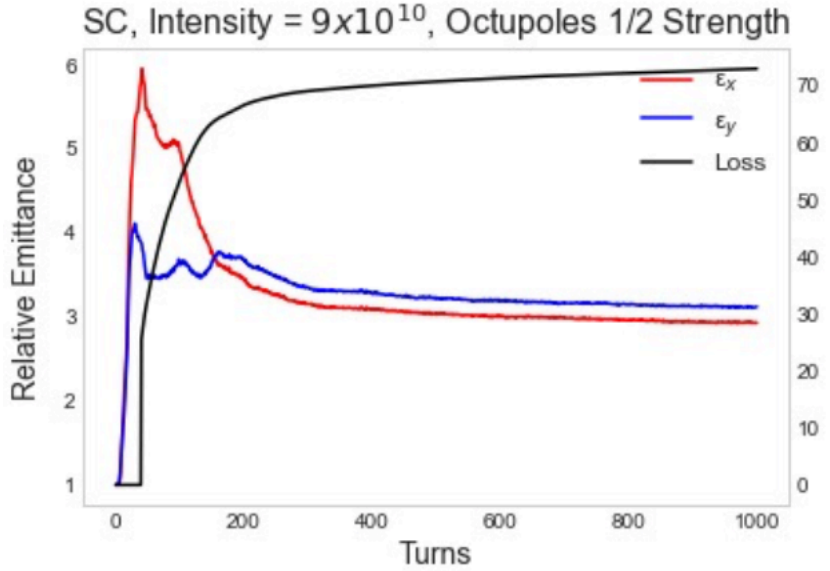

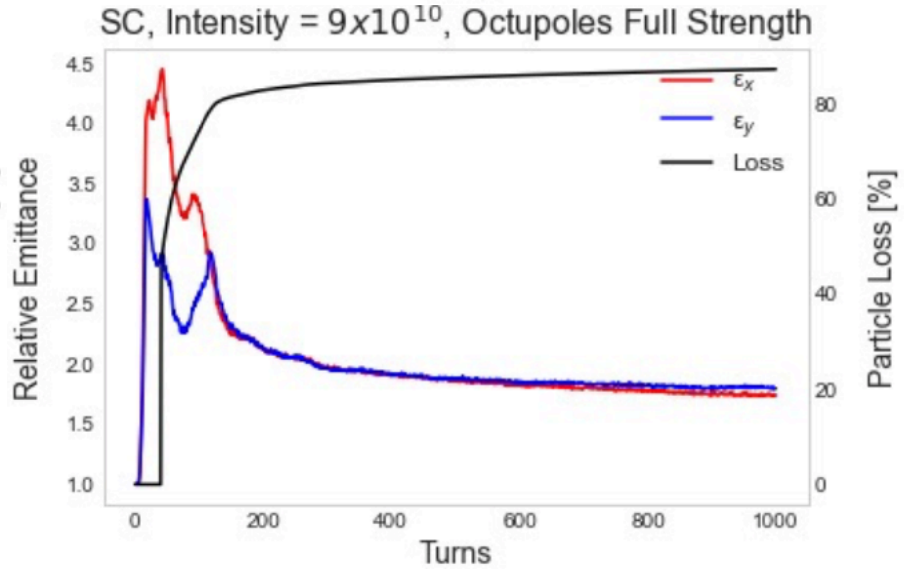

Part III: Space charge with a coasting beam

16

Coasting beam setup

- Transverse gaussian distribution with unnormalized emittance 4.11um
- Longitudinal coasting beam with dE uniformly in +-10keV and z uniformly in +-lattice length / 2
- RF Cavity has been removed
- All tracking uses pyORBIT 2.5D space charge solver with
  - 1M macro particles
  - grid size 128x128x1
  - 63 SC kicks per betatron wavelength

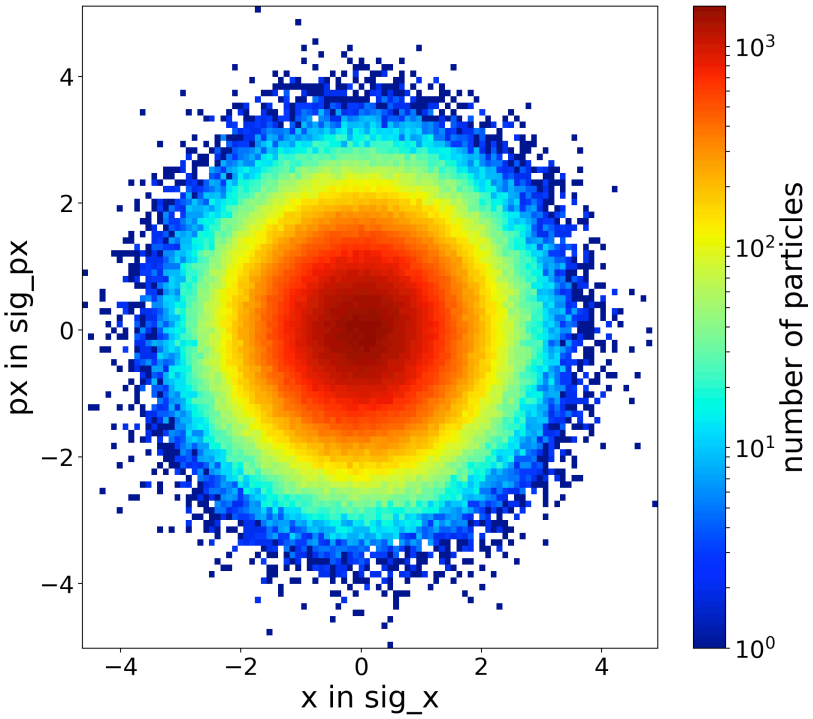

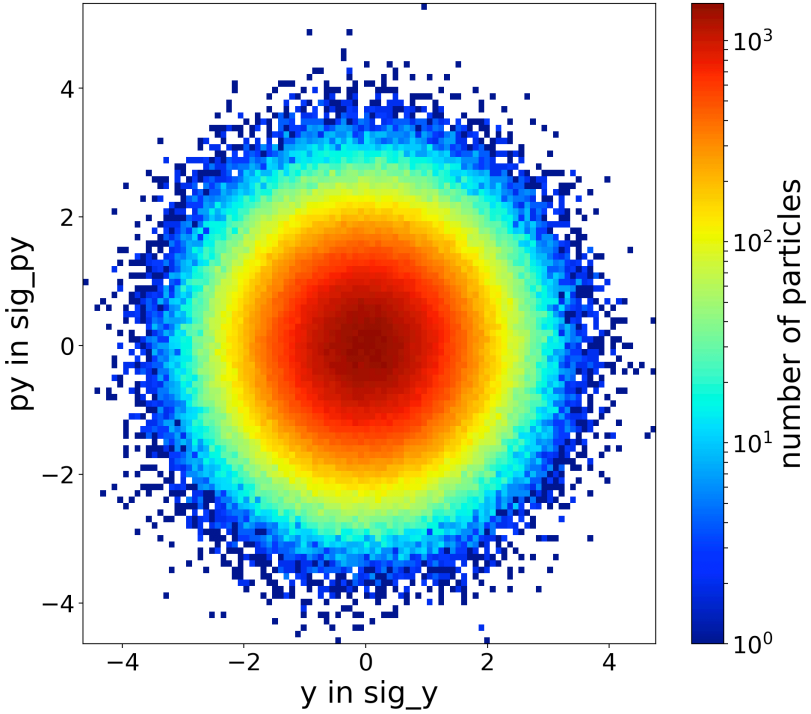

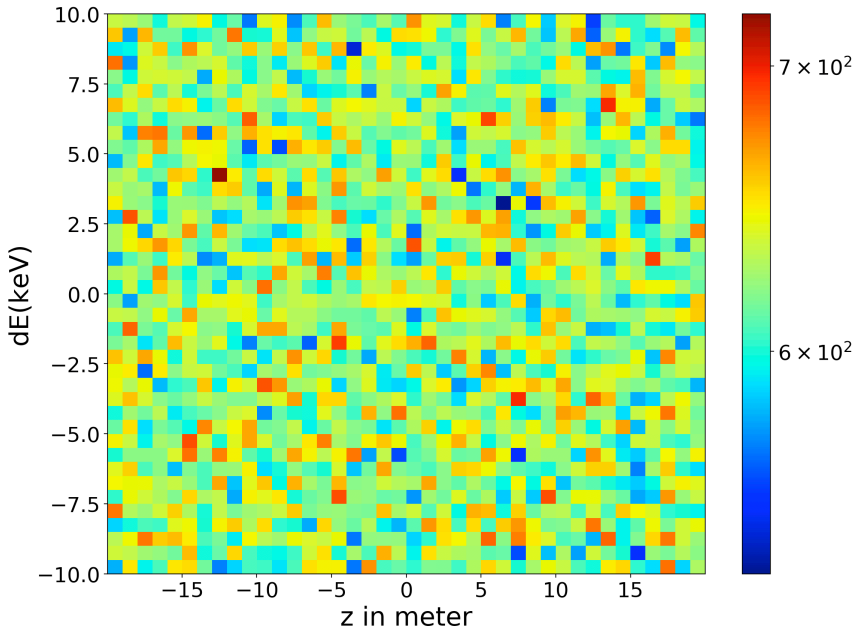

0 Amplitude Tune Shift and Tune Footprint

Following the same procedure as in bunched beam case, we compared the analytical 0 amplitude tune shift and tune footprint against theory

Normalized ϵ_x when stable	dQx at 0 amplitude
0.331 mm-mrad	-0.453

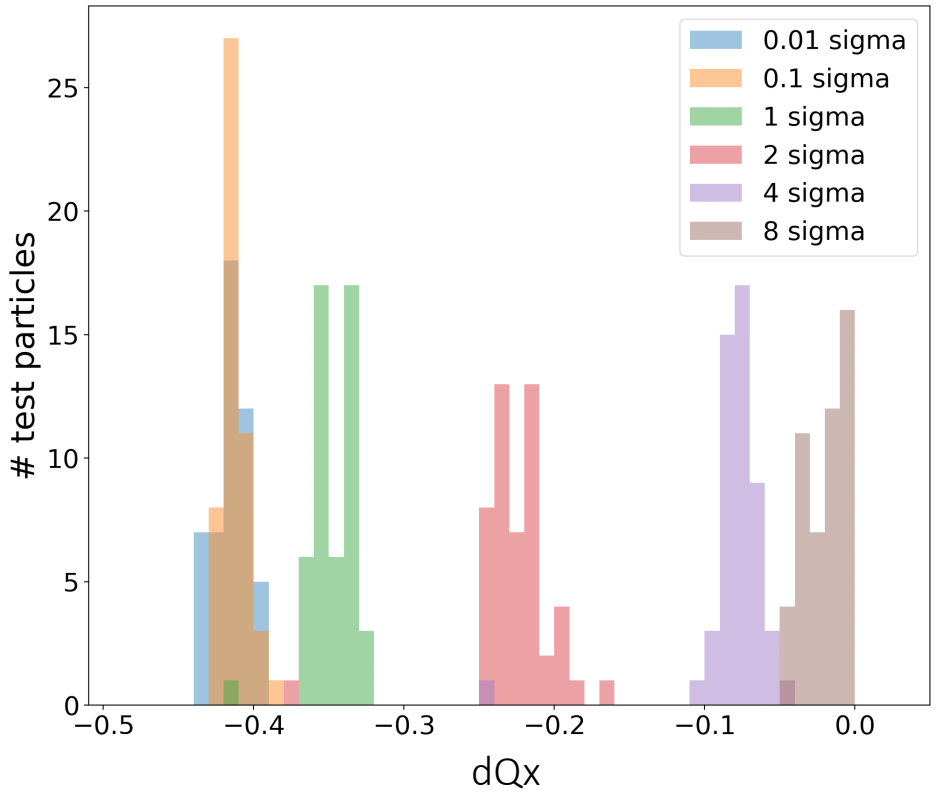

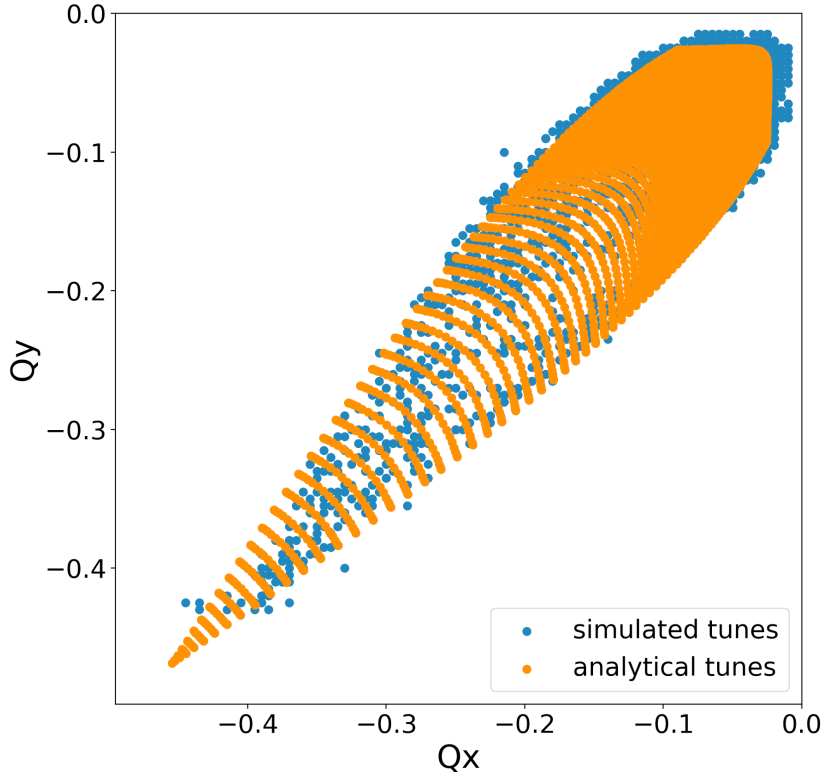

Initial Particle Loss with Realistic Aperture

- With space charge on, 40 turns of slow initialization, and realistic apertures set to 25mm everywhere in the ring except in the insert region (Min size x = 3.94mm y = 5.26mm), particle loss vs turn no is plotted. The initial particle loss is about 8.5%

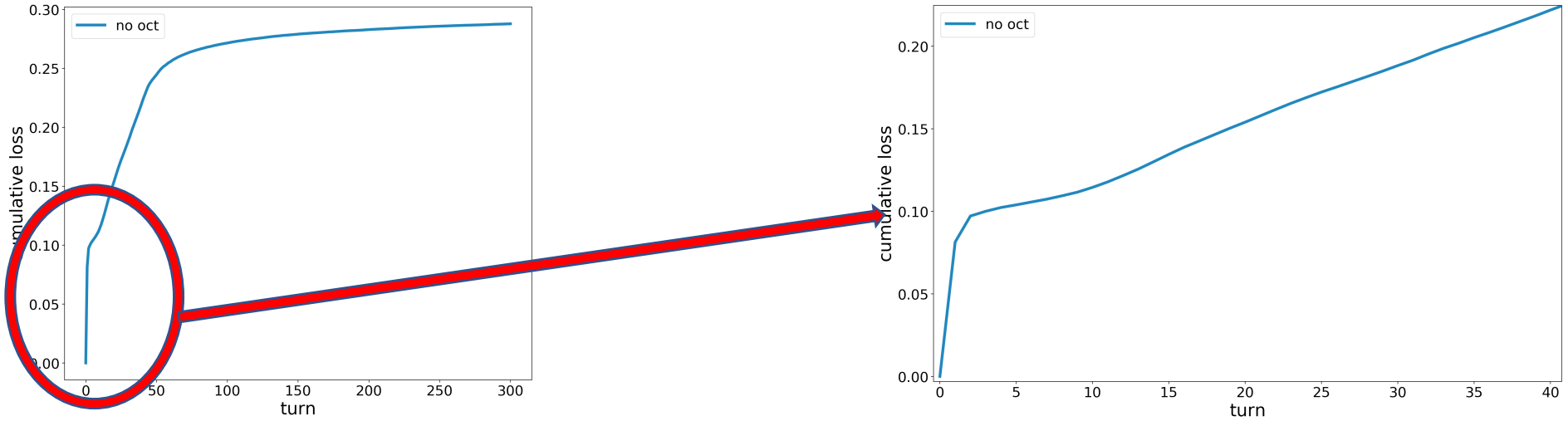

- The theoretically particle loss is obtained by integrating the fraction of particles outside the smallest aperture, according to this equation where θ_c is angle POA

$$f_L = \frac{2}{\pi}\left(\int_0^{\theta_C} \exp[-r_e(\theta)^2/(2\sigma^2)]\, d\theta - \theta_C \exp[-R_b^2/(2\sigma^2)]\right)$$

- We find f_L = 0.085 in agreement with the simulation.

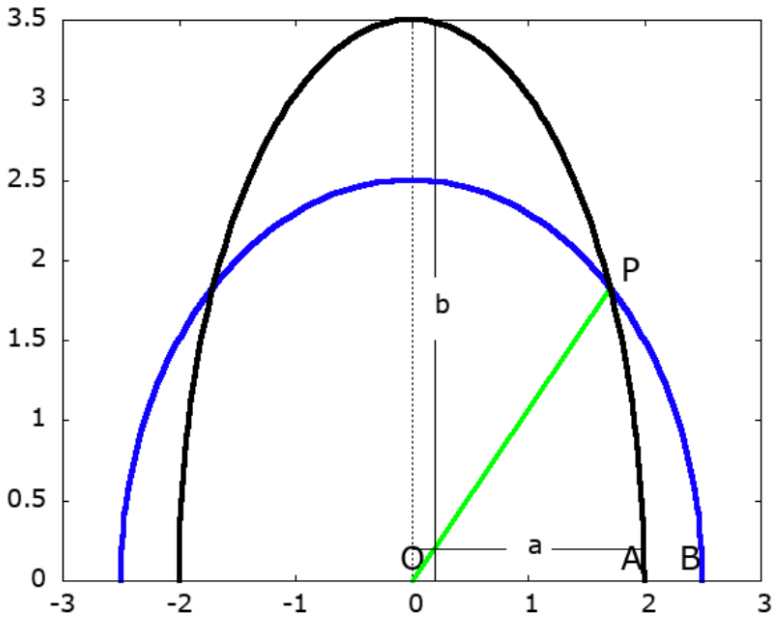

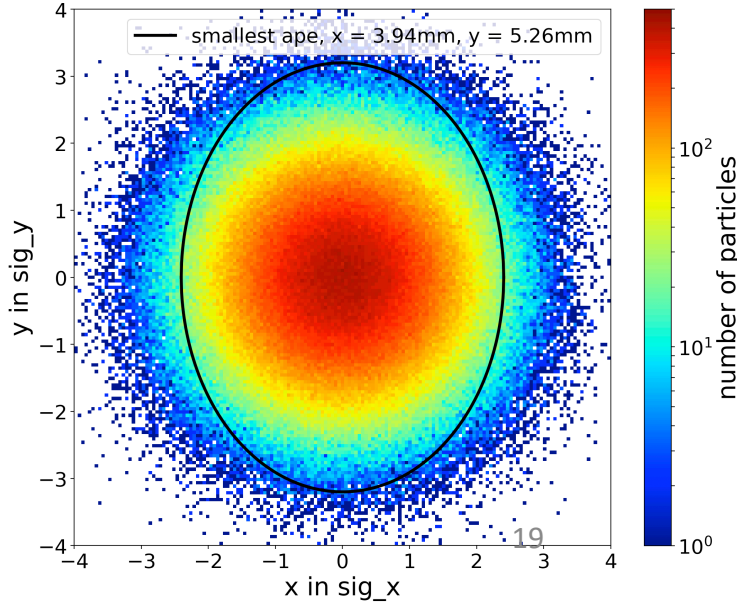

Dynamic Aperture with Octupoles and Realistic Aperture

- Octupoles are added with full strength, ½ strength, or ¼ strength, and realistic apertures are used
- The dynamic aperture obtained at all octupole strengths are similar due to the small realistic aperture

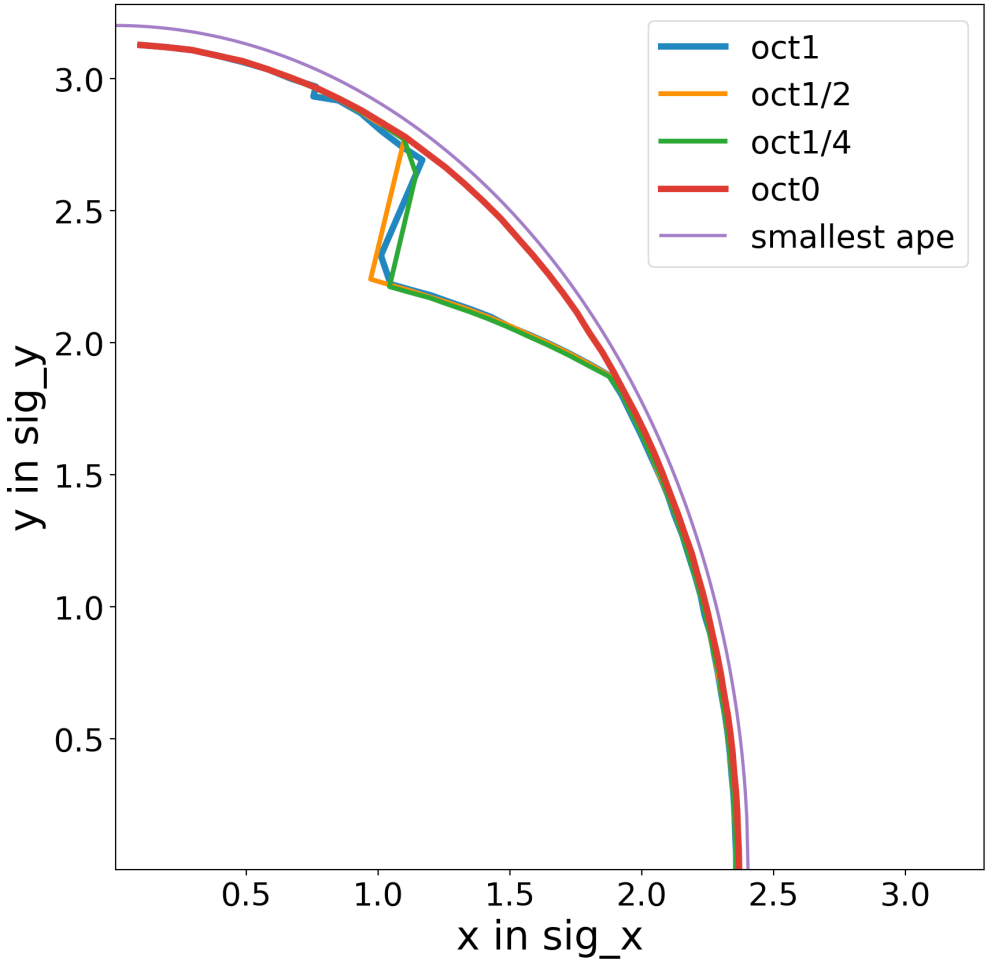

Emittance Evolution and Particle Loss with Octupoles and Realistic Aperture

- With SC, realistic aperture, and 40 turns of slow initialization, emittance evolution and particle loss are presented for 0, ¼, ½ and full octupole strength
- The particle loss and emittance variation at ¼ octupole strength is close to the case with no octupoles
- With octupole at full strength, the total loss is 37%, much less than for a bunched beam

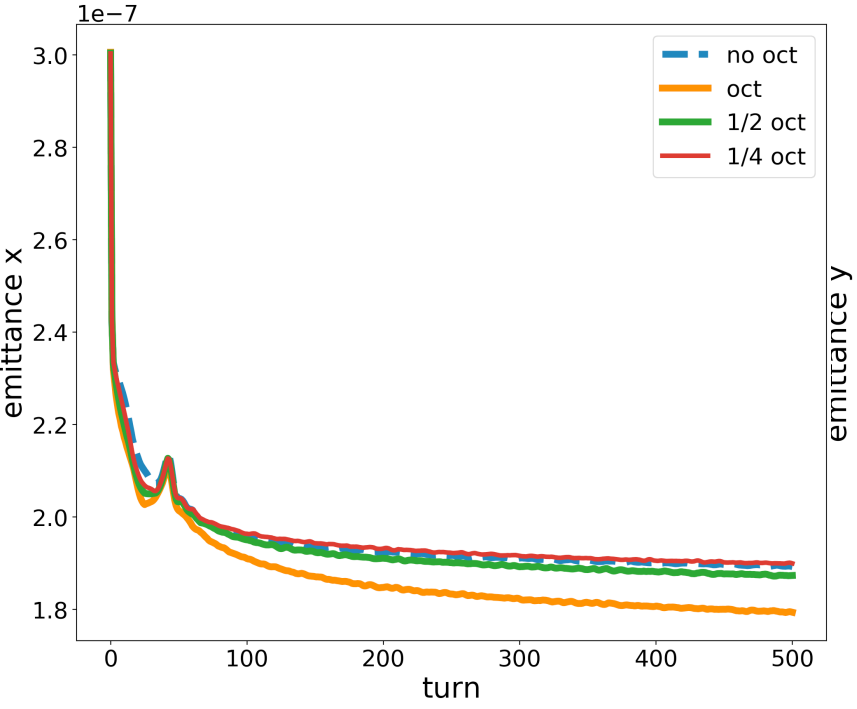

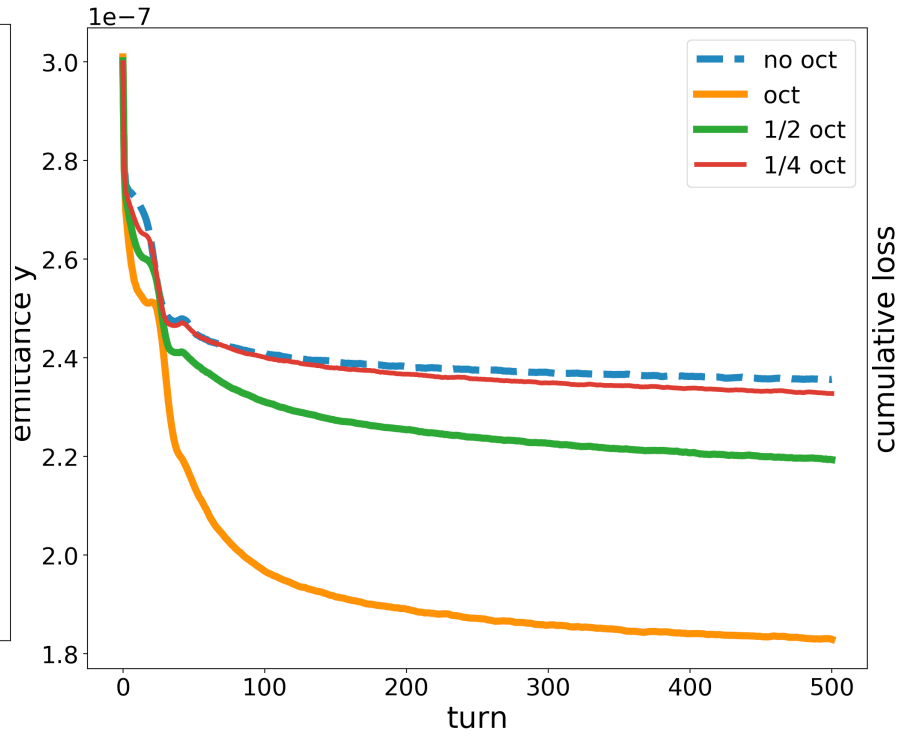

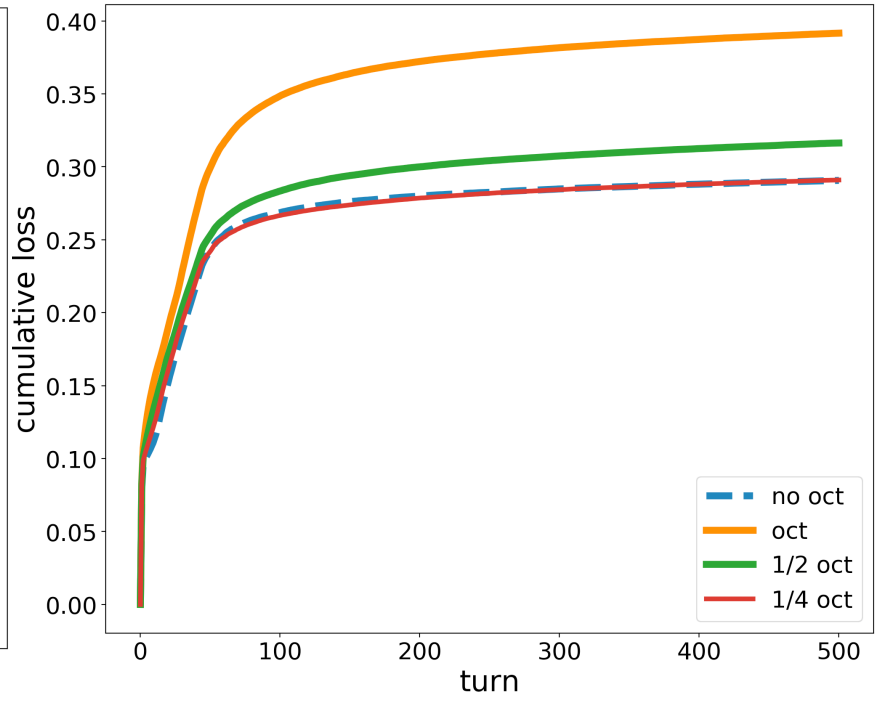

Part IV: Emittance Growth and RMS matching

Relevant Sources of Emittance Growth

- Nonstationary beam distribution
  - Stationary distribution retains it shape as it moves about the accelerator
  - Determined by forces acting on beam and self forces
  - Stationary if distribution is any function of beam Hamiltonian $\rho = f(H(\mathbf{x}, \mathbf{p}))$
  - Ex: KV distribution $\rho \propto \delta(E - H(\mathbf{x}, \mathbf{p}))$ uniform density in any plane
  - Gaussian distribution is nonstationary in a linear lattice, so emittance will grow

- Mismatched beam size
  - RMS beam size needs to be matched to lattice for beam size to remain stationary, which is determined by solutions to envelope equation
  - Both a mismatched KV or Gaussian beam will experience emittance growth
  - If KV and Gaussian beam of equivalent RMS sizes experience similar emittance growth, this would suggest that mismatch is the dominant source of growth

- Coupling from longitudinal to transverse plane
  - Dispersion and chromaticity are coupling sources

Emittance Growth Theory

- A beam is matched if its emittance is stationary. There is a perfect balance between the external focusing force, the space charge force, and the emittance term, shown in the envelope equation

$$k_0^2 a - \frac{K_{sc}}{a} - \frac{\epsilon^2}{a^3} = 0$$

$$a = 2x_{rms} \quad k_0 = Q/R$$

$$K_{sc} = \frac{e\lambda_L}{2\pi\epsilon_0\beta\gamma^2 pc}$$

$$\lambda_L = \frac{N}{2\sqrt{2\pi}\sigma_z}, \quad \text{Bunched beam}$$

$$\lambda_L = \frac{N}{C}, \quad \text{Coasting beam}$$

- If the beam is mismatched, there will be increased field energy, and the emittance will evolve. If the space charge (second) term dominates (greater than the third emittance term), the beam may grow without bound.

- Transition between emittance dominated and space charge dominated behavior occurs at a tune depression (tune with space charge/tune without space charge) of ~ 0.7

$$K_{sc} = k_i^2 a^2 \Rightarrow a^2(k_0^2 - k_i^2) = k_i^2 a^2$$

$$\frac{k_i}{k_0} = \sqrt{\frac{1}{2}} \approx 0.707$$

- Coasting beams in IOTA are not space charge dominated even at full intensity, and bunched beams become space charge dominated at intensities > 4 x 10^{10}

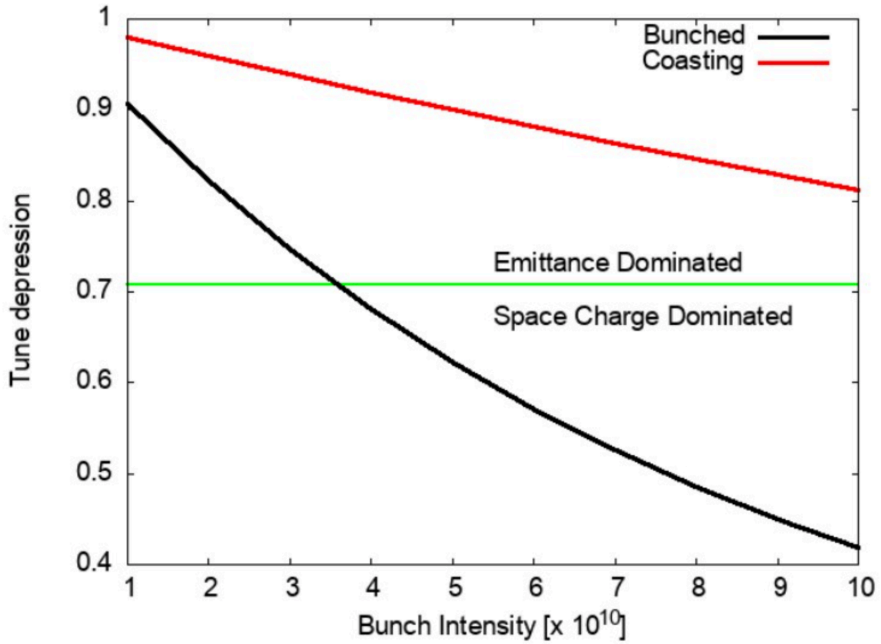

Emittance Growth Theory

- Key Assumption: smooth focusing and perfect axial symmetry in the x-y plane

- If the beam has an RMS size a_0 that is different from the matched beam size a_i for the same emittance, the excess energy due to the mismatch can be thermalized. The beam will then relax to a matched final state with an increased emittance

- Using the conservation of energy in the transverse planes, we can relate the relative change in emittance to the relative change in beam size

$$\frac{\epsilon_f}{\epsilon_i} = \frac{a_f}{a_i}\left[1 + \frac{k_0^2}{k_i^2}\{(\frac{a_f}{a_i})^2 - 1\}\right]^{1/2}$$

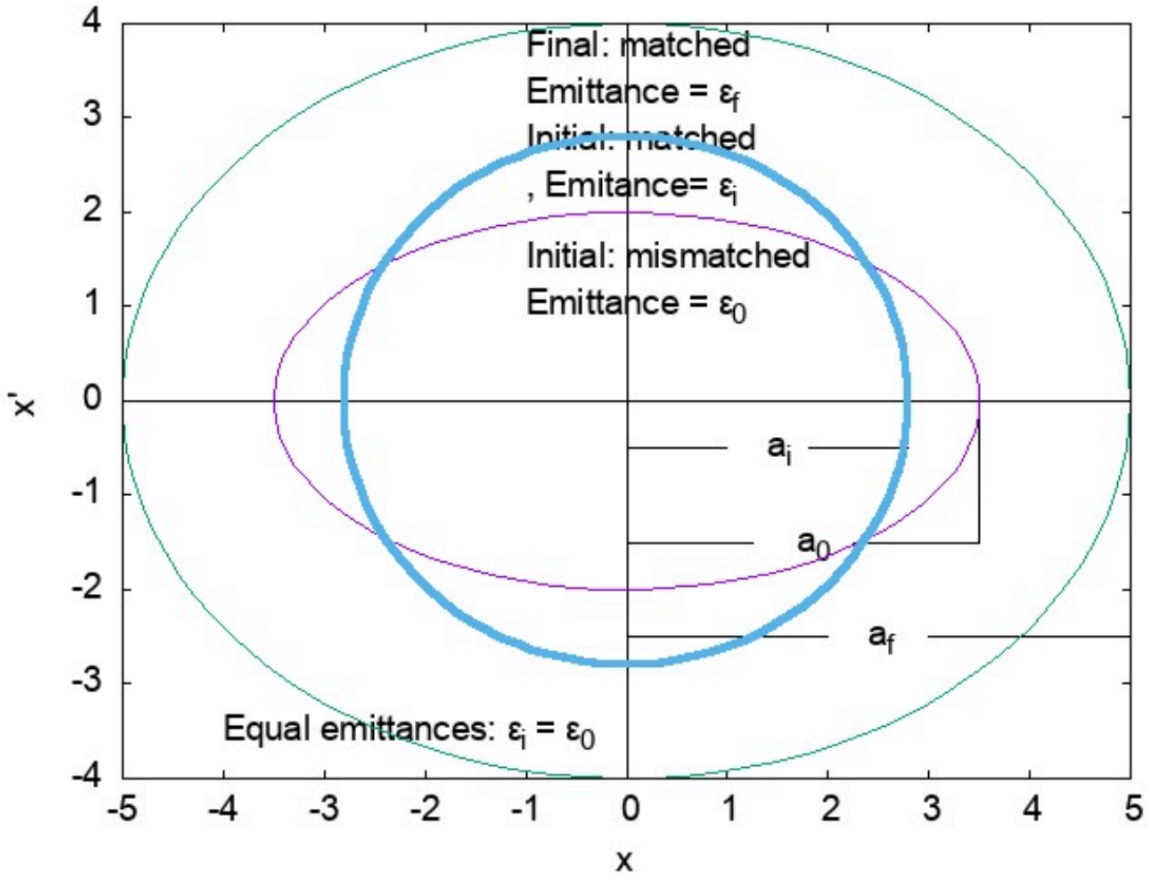

*M. Reiser, *J. App. Phys.*, 70, 1919 (1991)

Coasting and Bunched Beam Emittance Growth

- The simulated emittance growth for a coasting beam agrees well with simplified 1D theory (within ~2%)
- For a bunched beam, the simplified 1D theory accounts for more than half of the growth at full intensity
- The remaining discrepancy is likely due conditions that deviate from the assumptions underlying the simplified theory: non-uniform focusing, presence of dispersion and transverse coupling etc

Coasting beam emittance growth

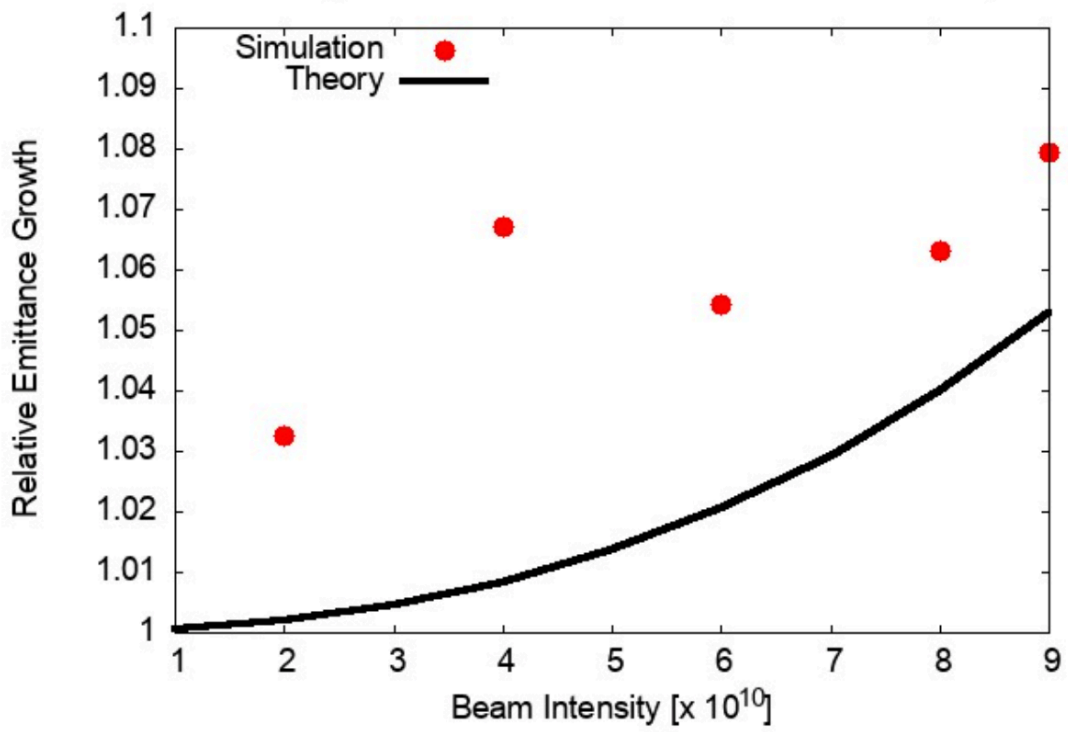

Bunched beam emittance growth

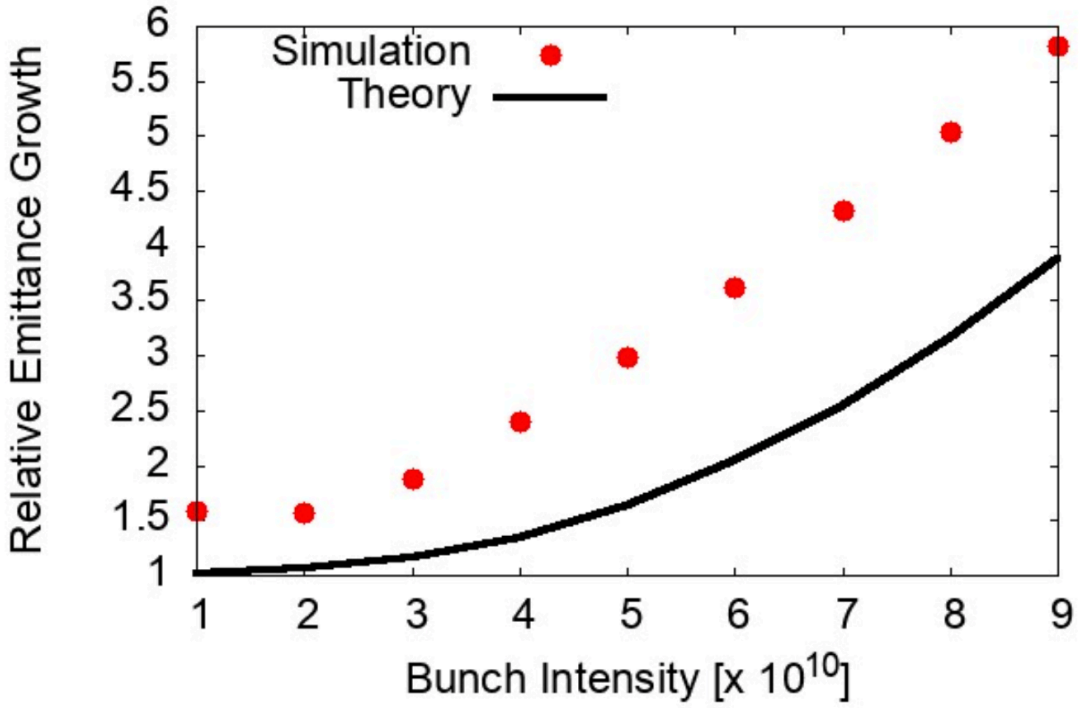

RMS Matching at Injection Point

- With bunched beam at full intensity 9e10, using physical aperture 0.1m and no octupoles, the beam is matched by optimizing the bunch beta parameter. The bunch is tracked for 1000 turns, and its emittance and particle loss in the end are recorded.
- Note that while matching could in principle be performed at any location, the choice of a high symmetry location reduces the no of parameters involved in the optimization.
- RMS matching is effective at reducing losses. In this particular case, for an optimally matched beam no loss was observed after 1000 turns. Optimum value found to be $\beta_{x,y}$ = 1.0 m
- Emittance is relatively insensitive to the quality of the RMS match

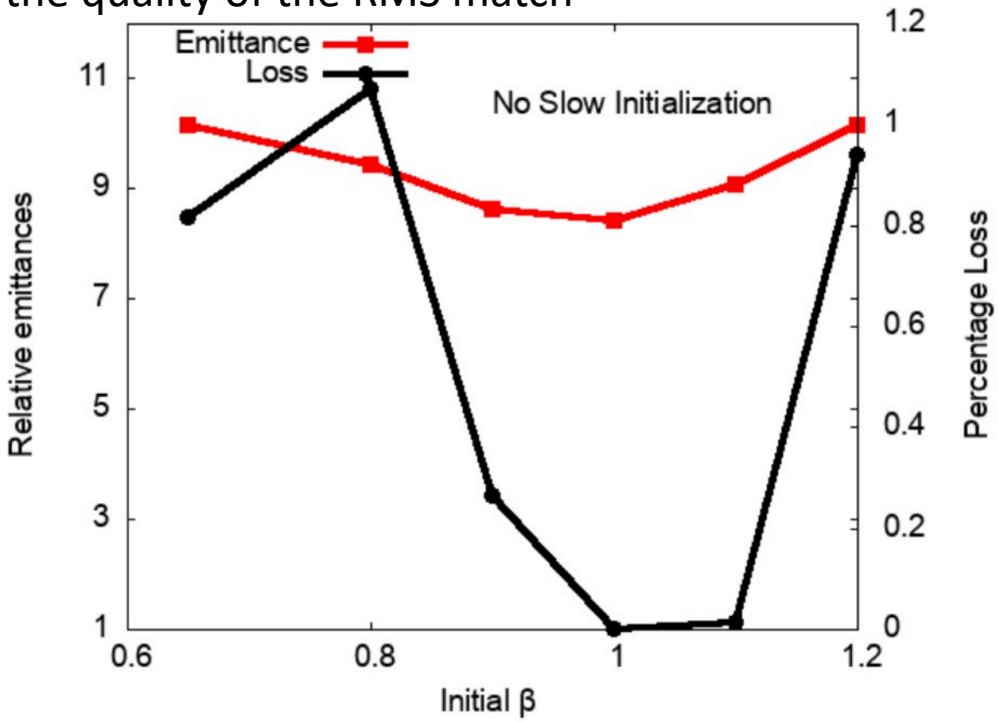

At injection point $\beta = \beta_x = \beta_y$

Ways to Minimize Early Beam Loss

- At fixed intensity, coasting beams have significantly lower loss (reduced space charge forces)
- Bunched beams
  - Operate in the emittance (not space charge) dominated regime , intensity < 4 x 10^{10}
  - At high intensities, slow initialization is effective at reducing initial emittance blowup and losses
  - Proper RMS matching is important. Under ideal conditions, losses can be suppressed
    - Requires confirmation under non-ideal conditions
  - With quasi-integrable (octupoles) or fully integrable (nonlinear lens) optics
    - Octupoles at ¼ strength do not increase losses
    - Increase aperture in octupoles
    - With either insert: space charge matched beam should maintain 2pi phase advance through the rest of the ring remains to be tested

Part V: Benchmarking pyORBIT with ImpactZ

Benchmarking ImpactZ and pyORBIT by Tracking Coasting Beam

- While Impact-Z (LBNL) provides a fully symplectic spectral solver, the PyORBIT FFT space charge solver is not symplectic. While ensemble averages (e.g. rms emittances) are expected to be in good agreement, meaningful differences may develop in the behavior of halo particles.
- The same initial distribution is used, which is generated by pyORBIT after stabilization
- The distribution is tracked for 10 turns with ImpactZ (Spectral 2D SC Solver) by Chad and with pyORBIT (FFT 2.5D Solver) by me. The H/V bunch sizes (in units of sigma) are recorded at every location around the ring during the final turn.
- The same bunch is tracked for 100 turns with pyORBIT and ImpactZ, and their emittance changes are compared. The results are in agreement at the 1% level

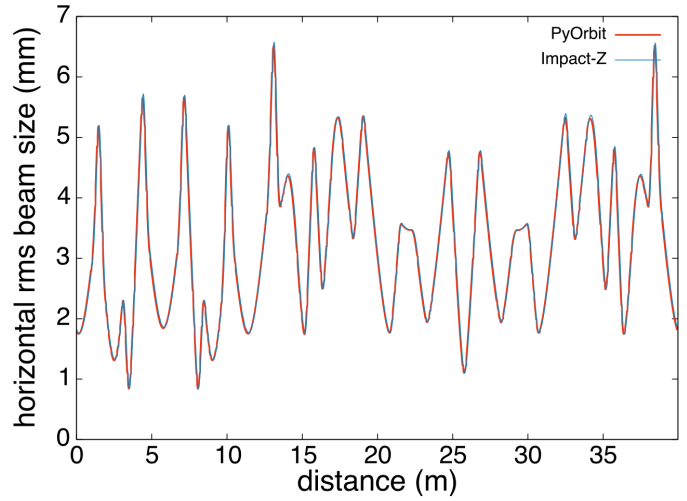

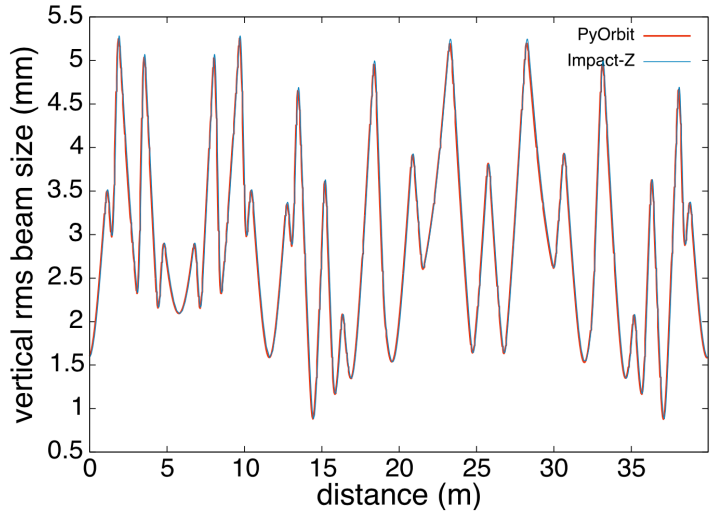

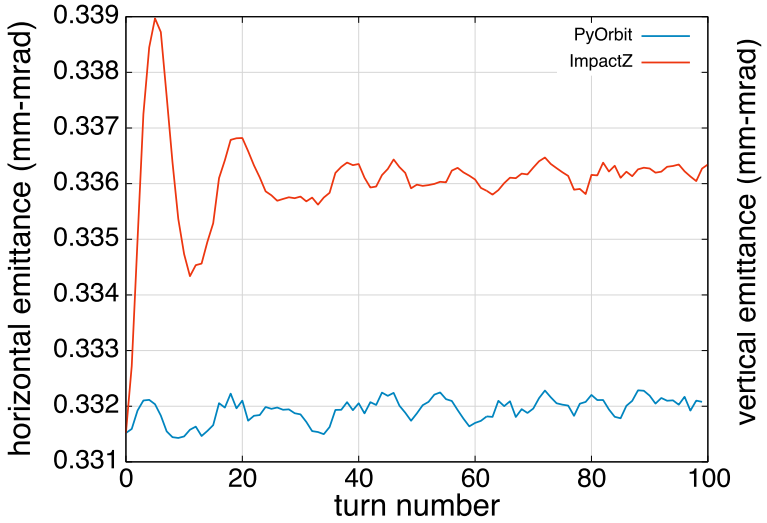

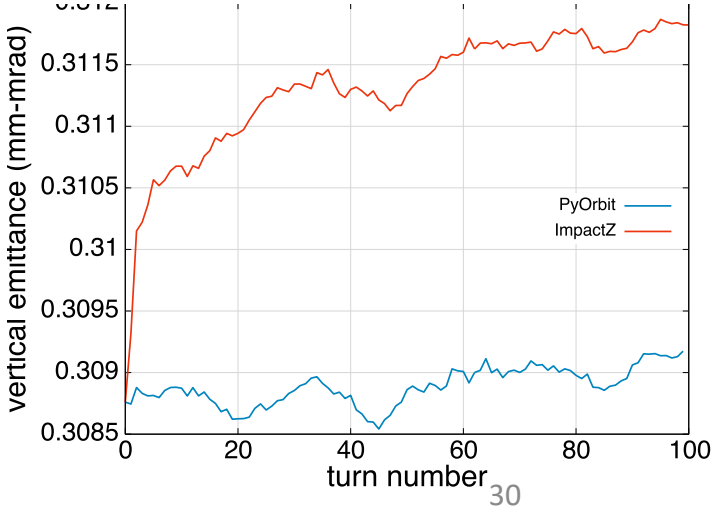

Conclusions

- Tests without space charge
  - Dynamic apertures obtained from pyORBIT and MADX agree well with each other
  - The tune footprint and dynamic aperture predicted by pyORBIT and MADX are very consistent
- Tests with space charge using longitudinal bunched beam
  - With space charge, slow initialization is performed to establish a steady state, with period set at 40 turns.
  - 0 amplitude tune shift and tune footprints agree well with analytical results
  - With octupole at full strength and aperture 0.1m, truncated bunch at full intensity (9e10) shows loss up to 80%
- Tests with space charge using longitudinal coasting beam
  - 0 amplitude tune shift and tune footprint agree well with analytical results
  - Initial particle loss with realistic aperture agrees well with analytical prediction
  - With octupole at full strength and realistic aperture, coasting beam at full intensity (9e10) shows loss up to 37%
- Emittance growth and RMS matching
  - For a coasting beam, the simplified emittance growth theory is in good agreement with simulations (within 2%), however, for a bunched beam it only explains half of emittance growth.
  - At full intensity (9e10), rms mismatch is a stronger source of emittance growth than the specifics of the initial distribution
  - Octupoles greatly reduce the dynamic aperture ($\sim 3\sigma$) and increase the particle loss
  - RMS matching is effective at reducing beam loss
- Rms beam size and emittance growth predicted by pyORBIT and ImpactZ are in very good agreement

Next Steps

- RMS matching with slow initialization: aim to minimize emittance growth and loss
- Improve the mismatch theory: Include 3D envelope equation with dispersion, transverse coupling, drop smooth focusing approximation, etc.
- Maintain integrability with space charge by matching phase advance to 2π through the rest of the ring
- Include longitudinal space charge forces
- Benchmarking pyORBIT with ImpactZ in tune calculations, emittance growth, and beam loss. Test different initial distributions

Backup Slides

Convergence Tests

- In pyORBIT, the accuracy of the space charge solver is mainly determined by the number of macroparticles (MP), the number of space charge kicks per betatron wavelength (N_{sc}), and the number of spatial grid points ($N_x \times N_y \times N_z$), which represent the beam while solving for the potential using Poisson's equation
- With two parameters fixed, the bunch is tracked with different values of the third parameter for 1000 turns, with 40 turns of slow initialization. The aperture is set to be 100mm.
- The relative emittance growth and percentage particle loss by the end of 1000 turns are used to check for convergence.
- As indicated in the following plots, #MPs = 500000, grid size 128x128x5, and N_{sc} = 63 are used as default parameters in all following tests

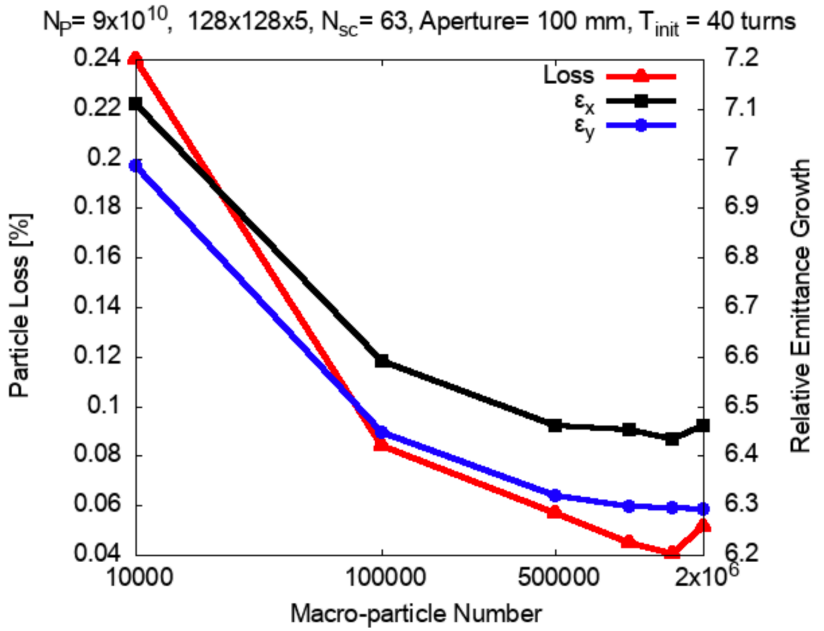

Particle loss (red) and relative emittance growth (black, blue) after 1000 turns as a function of the number of macro-particles

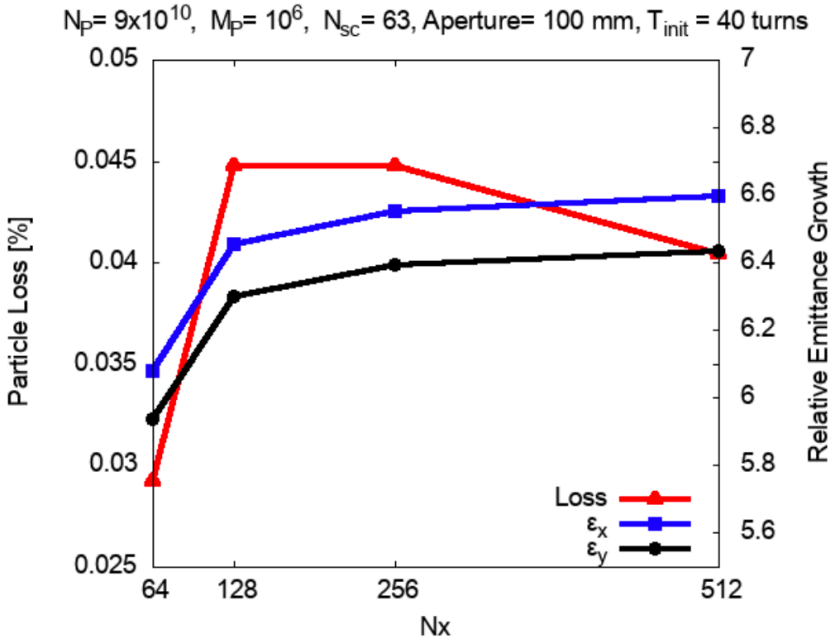

Particle loss (red) and relative emittance growth (black, blue) after 1000 turns as a function of grid size in x-y plane (N_x = N_y and N_z is fixed to be 5)

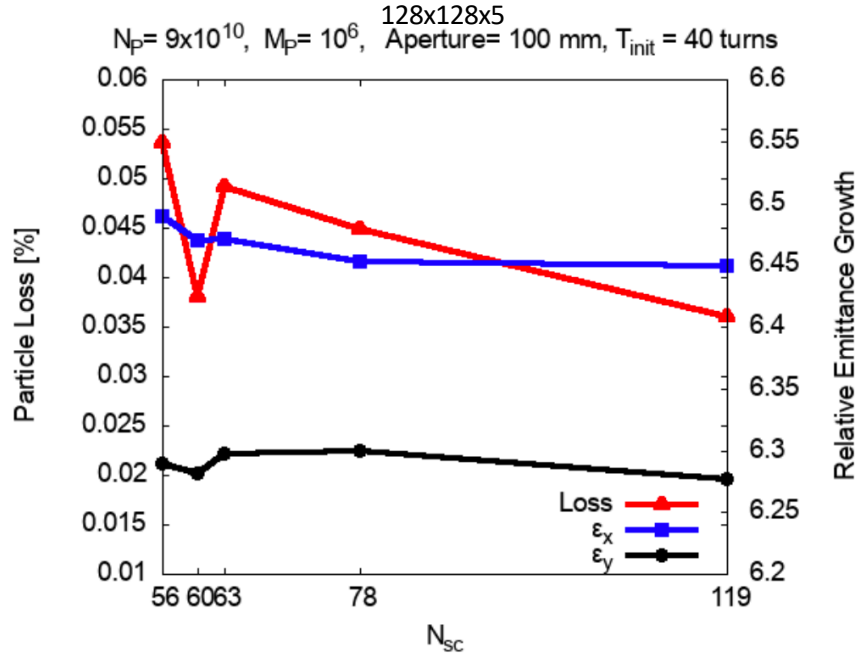

Particle loss (red) and relative emittance growth (black, blue) after 1000 turns as a function of number of space charge kicks per betatron wavelength

Changes Made to pyORBIT

- A new custom dipole edge element was added to pyORBIT. It accepts the same parameters as a dipole edge in MADX and uses the following transfer matrix

$$\begin{bmatrix} x \\ x' \end{bmatrix} = M = \begin{bmatrix} 1 & 0 \\ h\tan(e) & 1 \end{bmatrix} \begin{bmatrix} x_0 \\ x'_0 \end{bmatrix}$$

$$\begin{bmatrix} y \\ y' \end{bmatrix} = M = \begin{bmatrix} 1 & 0 \\ -h\tan(e-\psi) & 1 \end{bmatrix} \begin{bmatrix} y_0 \\ y'_0 \end{bmatrix}$$

$$\psi = \mathtt{fint} \cdot 2 \cdot \mathtt{hgap} \cdot h \cdot \frac{1+\sin^2(e)}{\cos(e)}$$

- In pyORBIT, all sources of nonlinearity, especially the magnet fringe effect, have been removed. The existence of magnet fringe effect in pyORBIT causes a 30% difference in single particle phase space diagram, as indicated in the following plot:

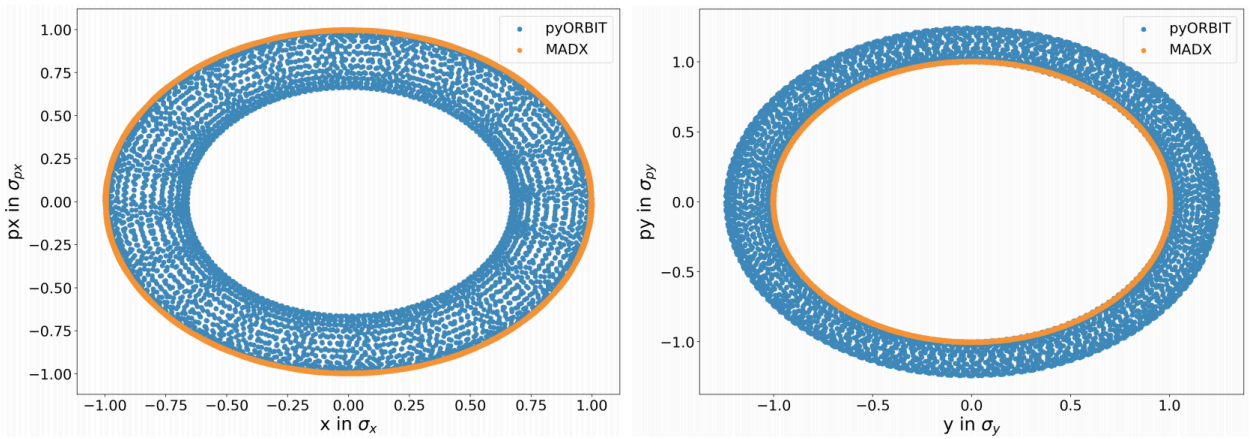

Single particle phase space diagram in pyORBIT and MADX without removing the pyORBIT magnet fringe effect

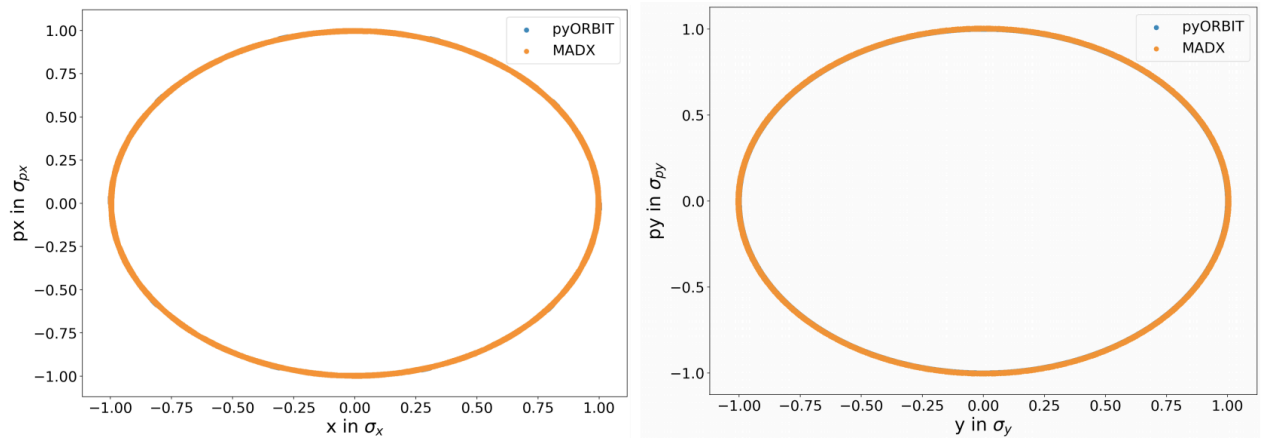

Single particle phase space diagram in pyORBIT and MADX after removing the pyORBIT magnet fringe effect

Symplecticity Test of Linear IOTA Lattice with and without Octupoles

- This test aims at assessing the symplecticity of particle tracking in IOTA using pyORBIT, for cases with and without octupoles
- All sources of nonlinearity other than the optional octupoles, like space charge and nonlinear effect in dipole and quadrupole, are turned off.
- For initial coordinates ($n*\sigma_x$, 0, $n*\sigma_y$, 0, 0, 0) n = 0, ..,5, we assign test particles in a close neighborhood (defined as $X_i \pm$ step_size $* \sigma_{Xi}$) to numerically calculate the elements of Jacobian transfer matrix $\frac{\partial X_i(s_f)}{\partial X_j(s_0)}$ where $X_j(s_0)$ and $X_i(s_f)$ are the initial and final (1-turn) phase space Floquet coordinates.
- For symplectic tracking, one expects detJ = 1 and $J^T S J = S$ (S is the symplectic matrix). As a measure for the latter condition, we use the maximum absolute value of the entries of the matrix $J^T S J - S$.

36

Linear IOTA Lattice (without Octupoles)

detJ – 1 test

	MADX	pyORBIT
Optimal derivative step size	0.01	0.01
Largest deviation	10^{-7}	10^{-11}

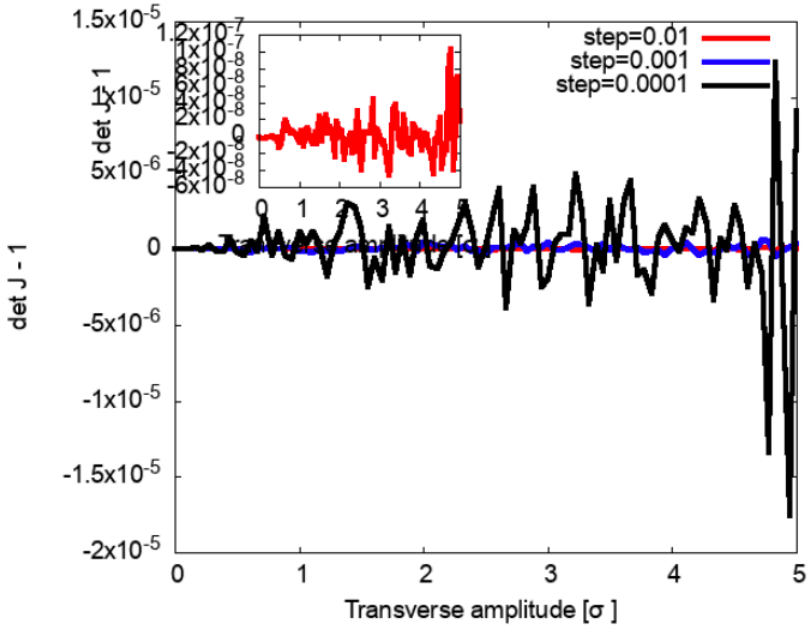

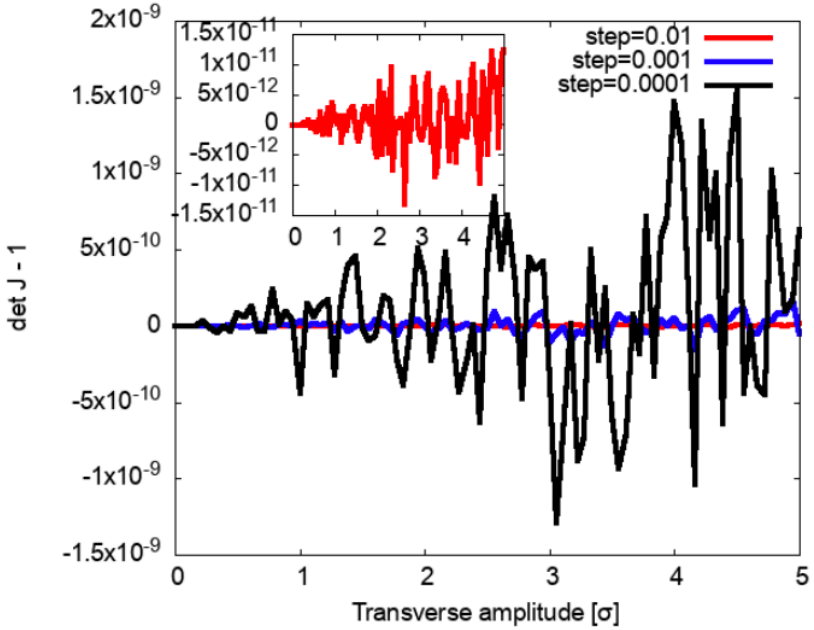

Determinant of J (n = 0 , …,5) for different step sizes calculated in MADX(left) and pyORBIT(right)

$|J^T S J - S|$ test

	MADX	pyORBIT
Optimal derivative step size	0.01	0.01
Largest deviation	10^{-8}	10^{-12}

In pyORBIT all sources of nonlinearity have been removed, while in MADX some residual nonlinearity exists in dipoles and quadrupoles.

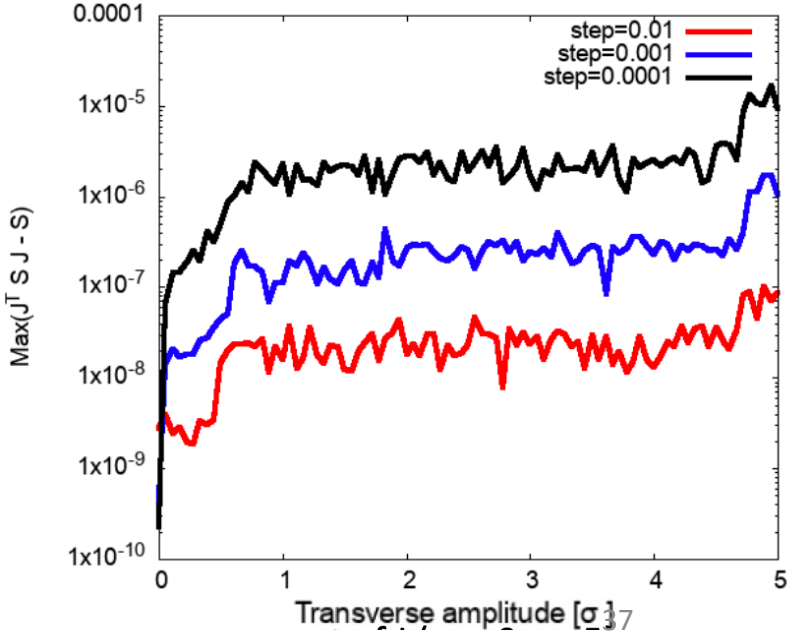

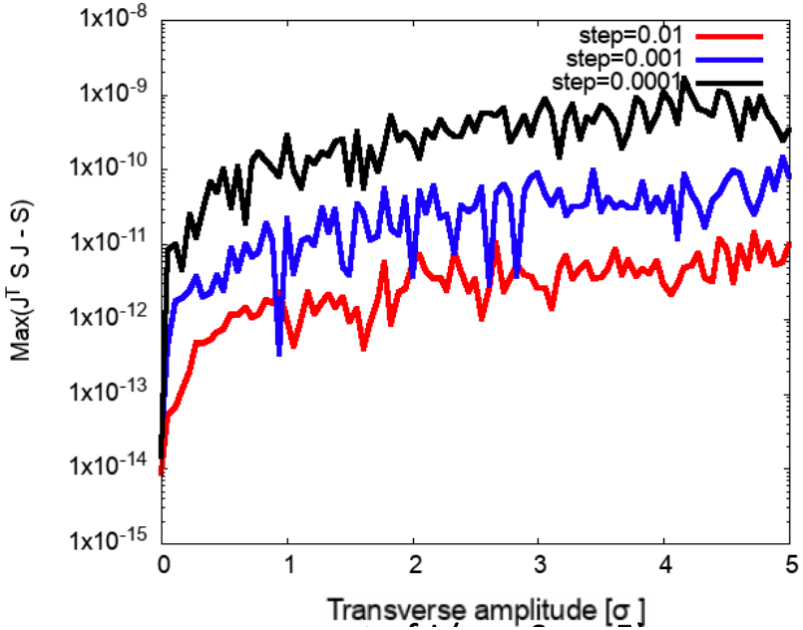

Max($J^T S J - S$) (n = 0,…,5) for different step sizes calculated in MADX(left) and pyORBIT(right)

IOTA Lattice with Octupoles

detJ - 1 test

	MADX	pyORBIT
Optimal step size	0.001	0.001
Largest deviation	10^{-4}	10^{-4}

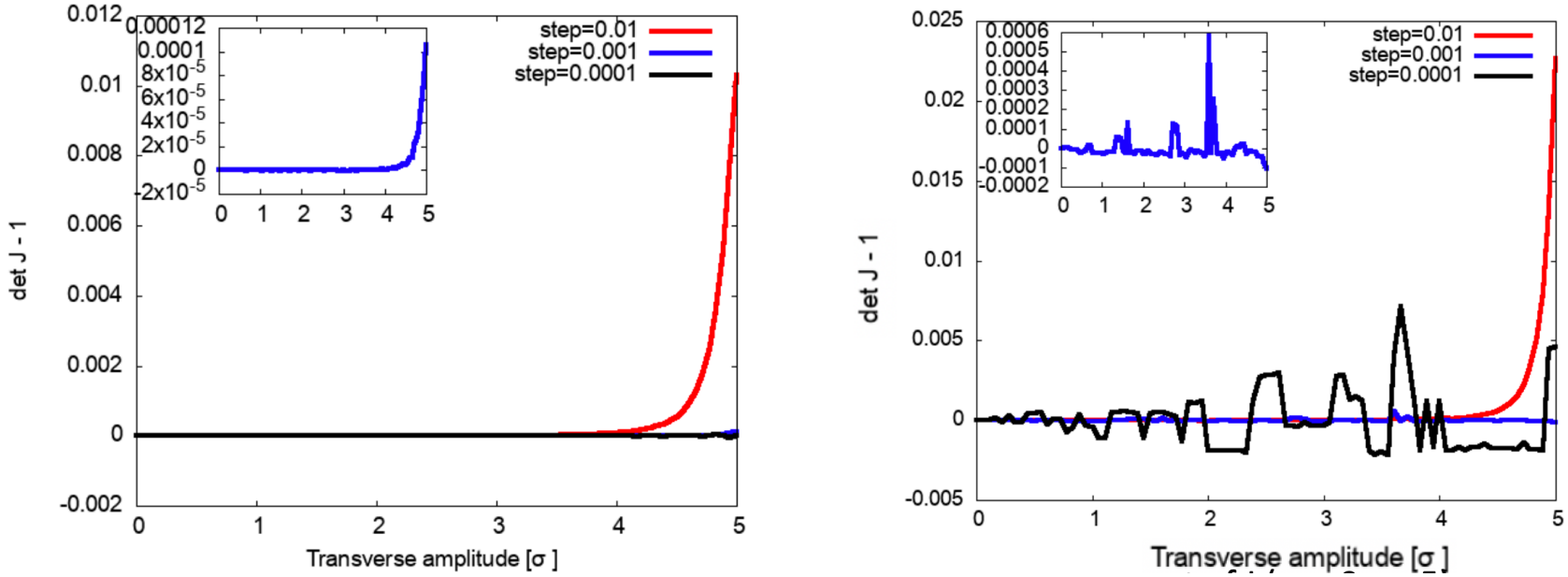

Determinant of J (n = 0 , …,5) for different step sizes calculated in MADX(left) and pyORBIT(right)

$|J^T S J - S|$ test

	MADX	pyORBIT
Optimal step size	0.001	0.001
Largest deviation	10^{-7}	10^{-5}

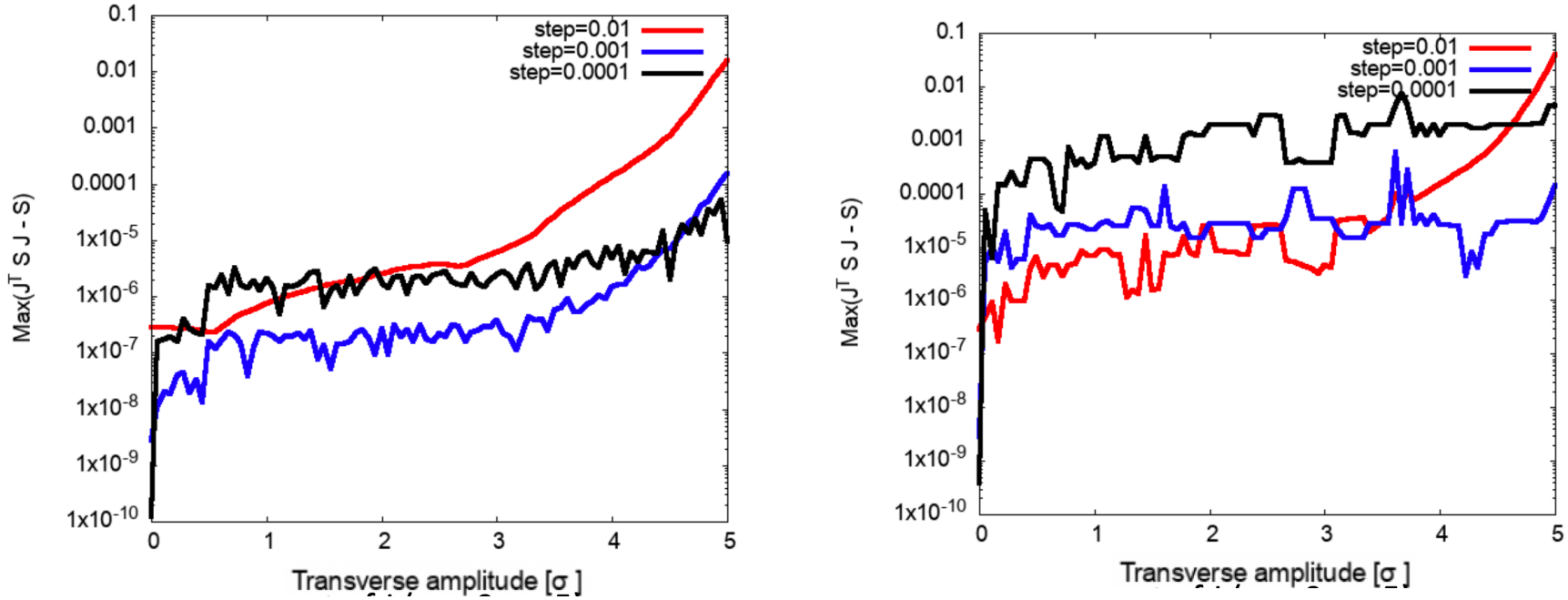

Max($J^T S J – S$) (n = 0,…,5) for different step sizes calculated in MADX(left) and pyORBIT(right)

Here octupoles are the dominating source of nonlinearity.

Symplecticity Test for Linear IOTA Lattice with Space Charge

- This test aims at assessing the symplecticity of particle tracking in IOTA with space charge effect using pyORBIT
- Intensity is 8mA, which corresponds to $9*10^{10}$ protons/bunch
- Procedure is similar to previous tests

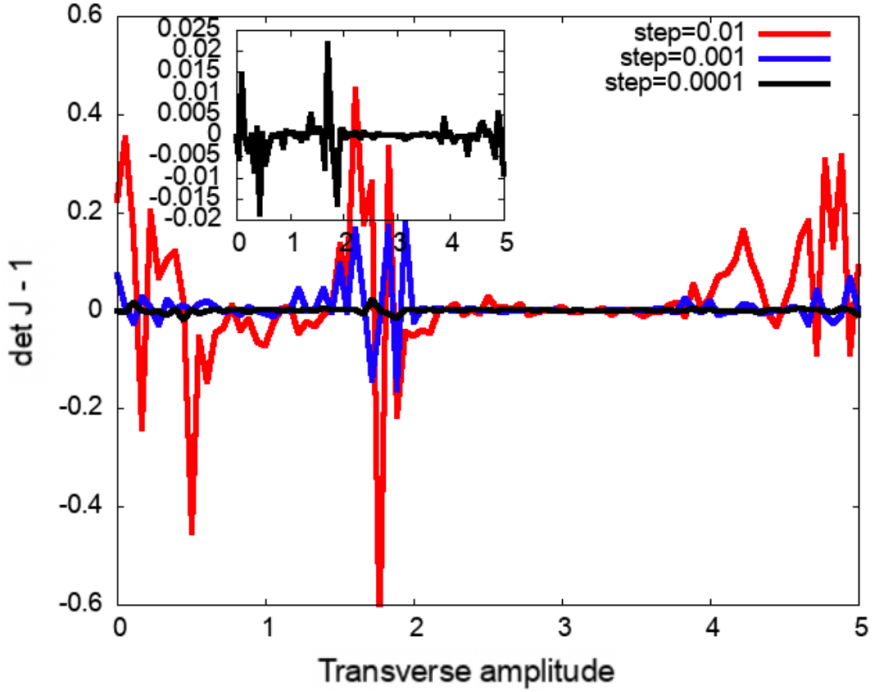

Determinant of J at n factor from 0 to 5 for different step sizes

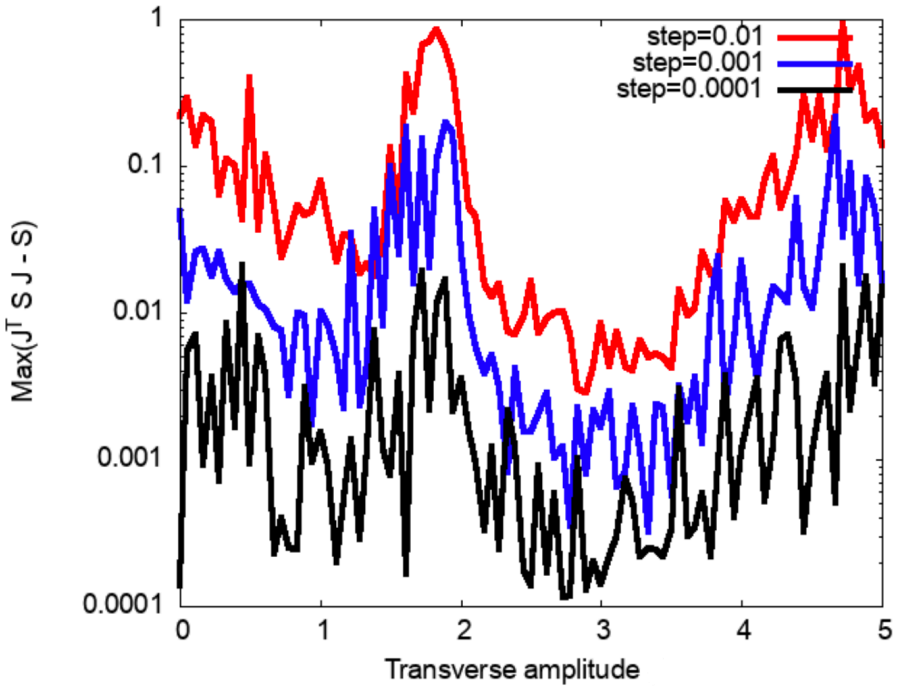

Maximum absolute value of elements in $J^T S J - S$ for n factor from 0 to 5 for different step sizes

- The best result comes from step size 0.0001, in which the largest deviation of detJ – 1 is 0.02 and the largest deviation of $|J^TSJ-S|$ is 0.01. The result also shows large deviation from 0 at amplitude close to 2σ
- We observe larger deviations from symplecticity in the presence of space charge. This is not unexpected since the pyORBIT space charge solver is not symplectic since due to interpolation using a finite grid.

39

Single Particle Hamiltonian Invariant for IOTA Lattice with Octupole Insert

- In the presence of an octupole insert, the theory predicts the existence a single Hamiltonian invariant:

$$H = \frac{1}{2}(p_{x,N}^2 + p_{yN}^2 + x_N^2 + y_N^2) + \frac{1}{24}\kappa[x_N^4 + y_N^4 - 6x_N^2 y_N^2]$$

where kappa is a constant.

- A test particle initialized at (0.5*σ_x , 0, 0.5* σ_y , 0, 0, 0), is tracked for 10000 turns in MADX and pyORBIT. Relative variations of H are plotted.

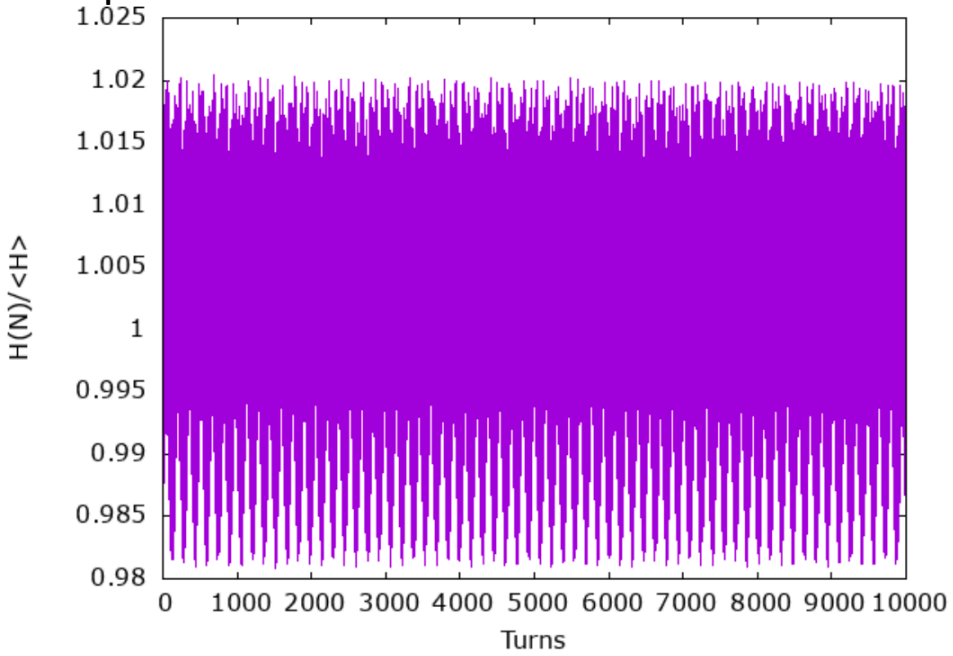

for MADX tracking result

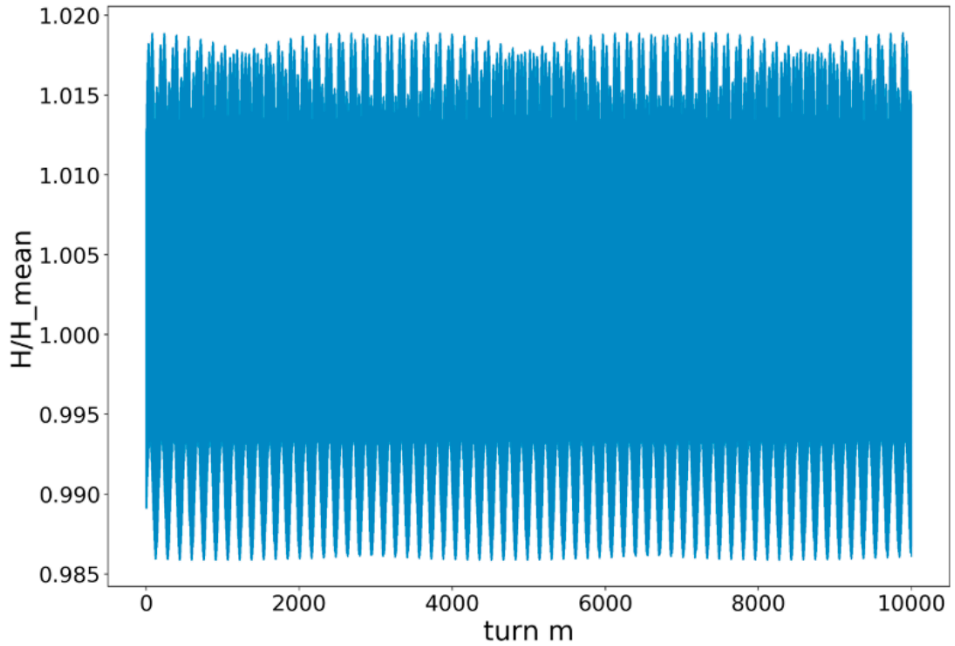

for pyORBIT tracking result

- MADX and pyORBIT both show fluctuations of ±2% (due to the division of ideal octupole longitudinal profile into 17 equally spaced segments). For particles initialized at larger amplitude, the fluctuations are somewhat larger, but the 2 codes remain in agreement.

40

Periodic Boundary Condition and Tracking Test

- A longitudinal periodic boundary condition is applied. At the start of each turn particles are moved so that -C/2 < z < C/2
- With a 40 turns slow initialization and aperture size 0.1m, the bunch is tracked for 500 turns. The initial and final z and dE distributions remain uniform as shown on the right plots.
- The bottom plot shows the evolutions of beta and relative emittances (5% in emit_y and 10% in emit_x)
- Particle loss is 0

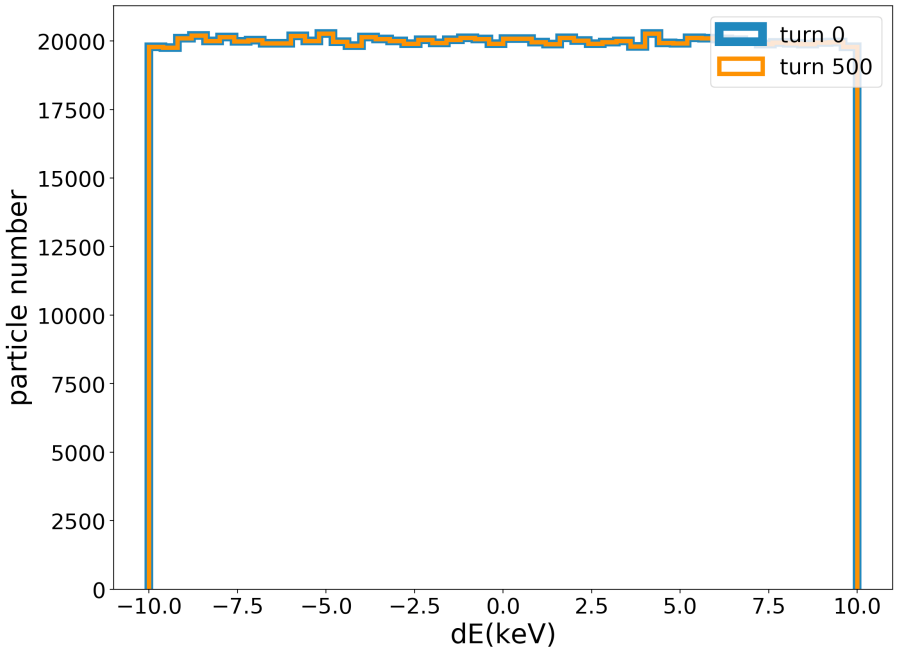

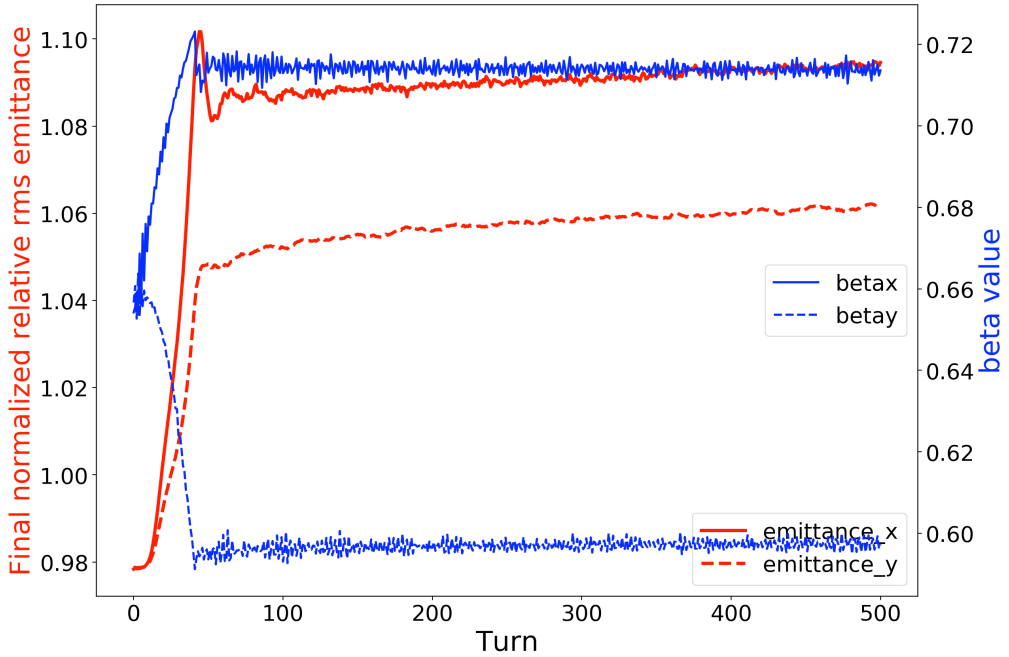

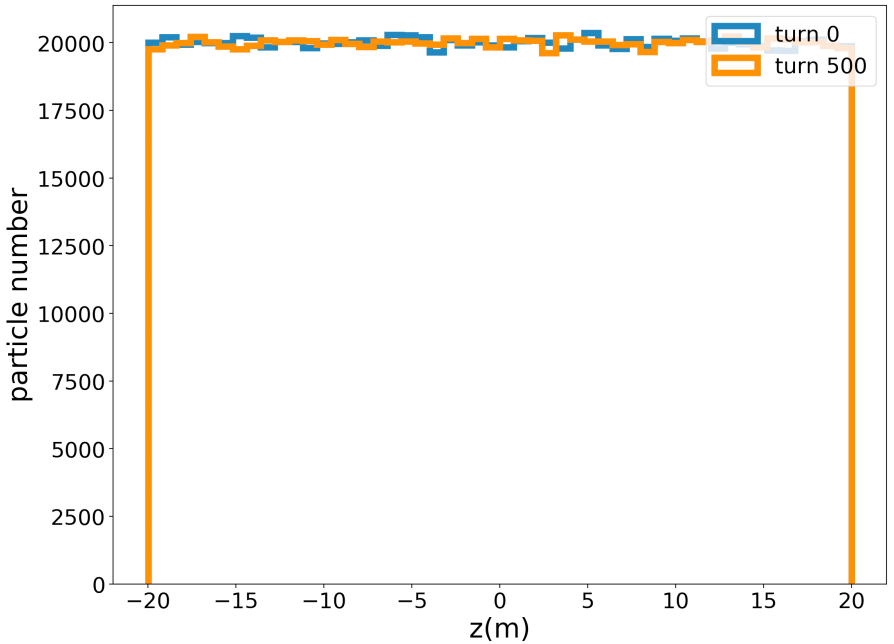

Emittance Evolution and Particle Loss with Realistic Apertures and Octupoles

Emittance growth and particle loss for:

- No octupole, no truncation
- Octupole with initial distribution cut at 3 sigma
- Octupole with initial distribution cut at 1.5 sigma

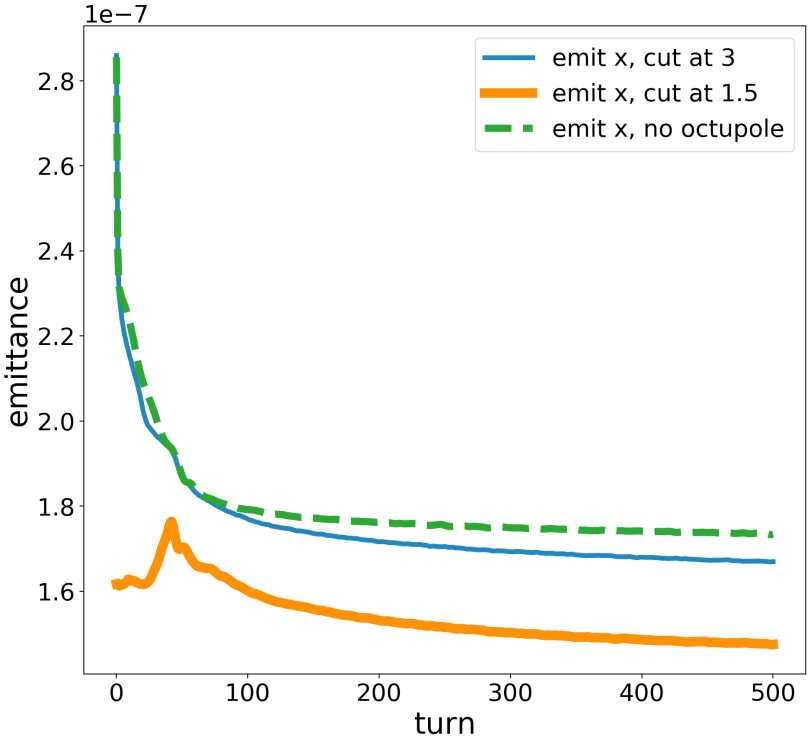

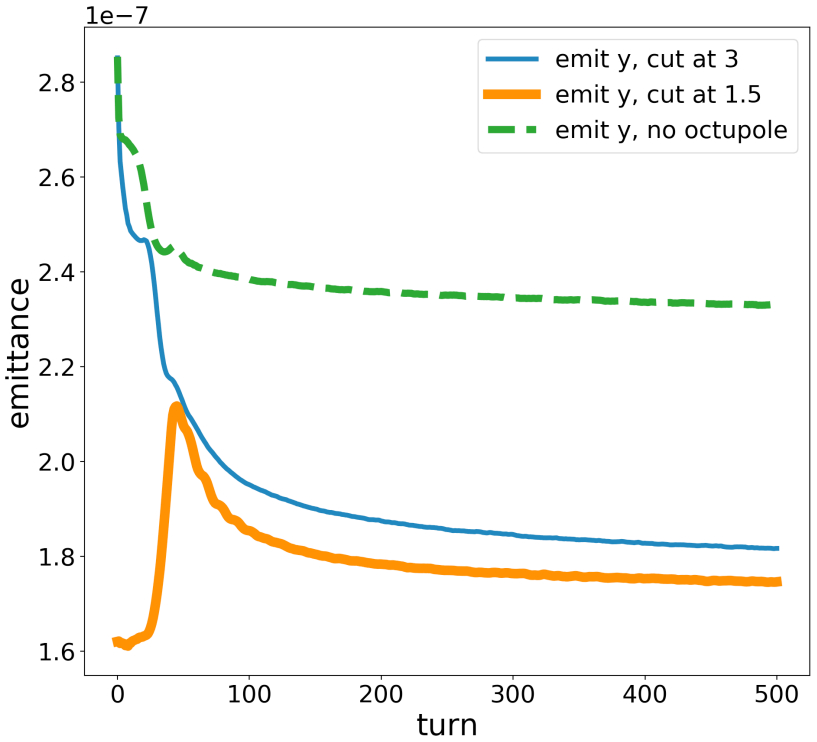

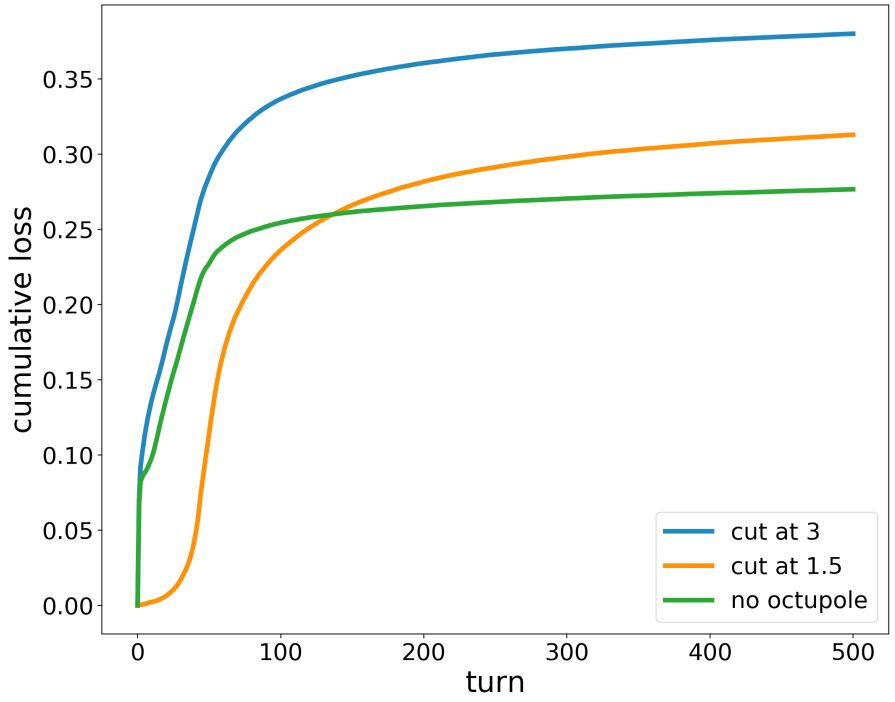

After trunacting at 1.5 sigma, emittance grows sharply until the bunch size reaches the physical aperture. It then decays due to particle losses and eventually stabilizes.

Truncating the initial distribution at 1.5 sigma results in reduced overall particle losses.

Beam evolution at turn 0, 100, 300, 500 for 3 cases

In all 3 cases, the particle distribution change is most significant during the first 100 turns due to slow initialization.

no octupole

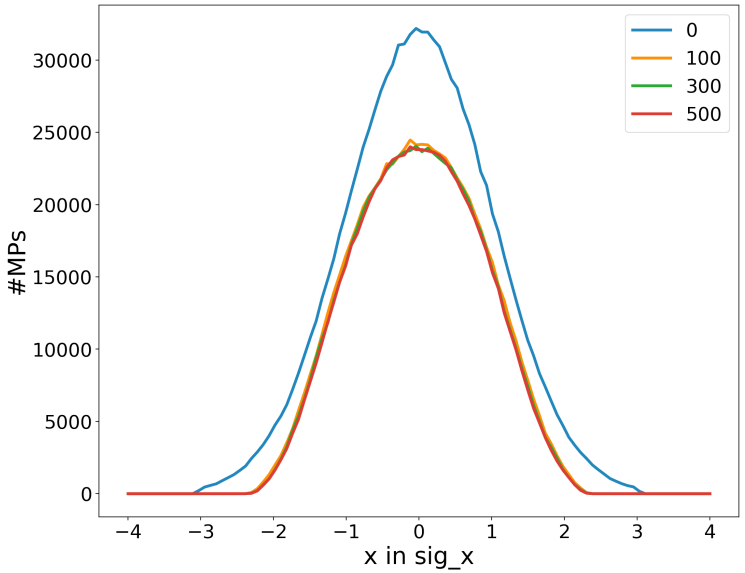

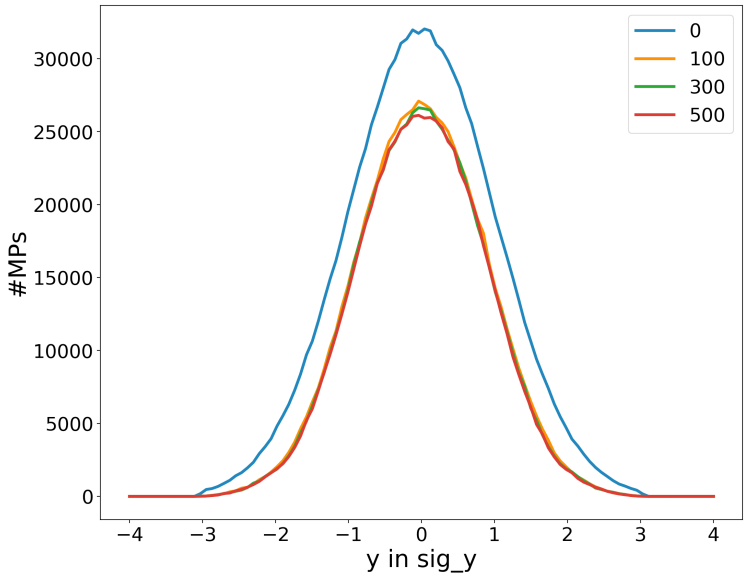

with octupole, cut at 3sigma

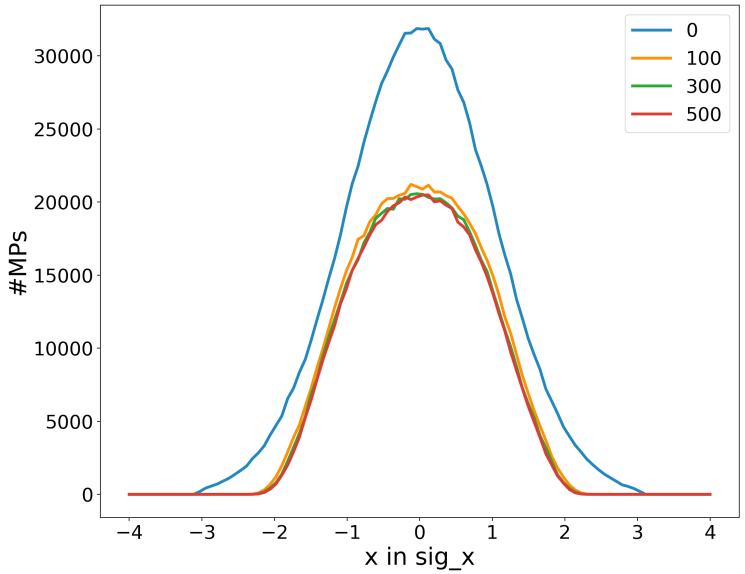

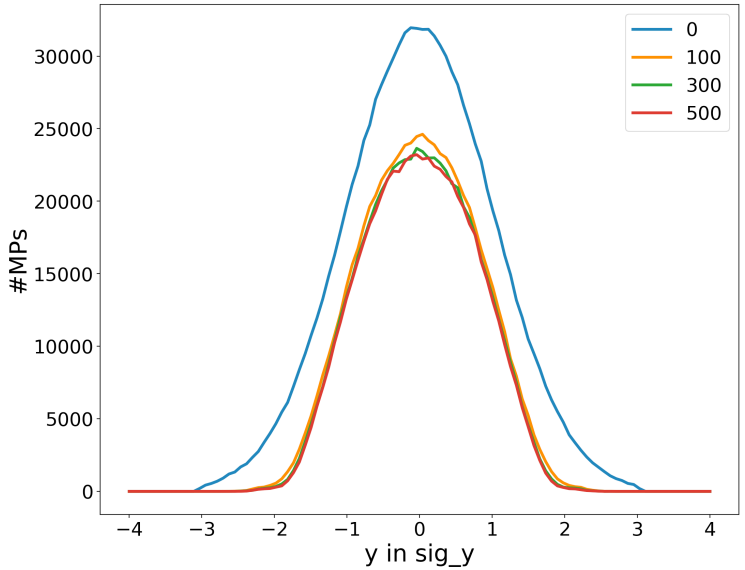

with octupole, cut at 1.5sigma

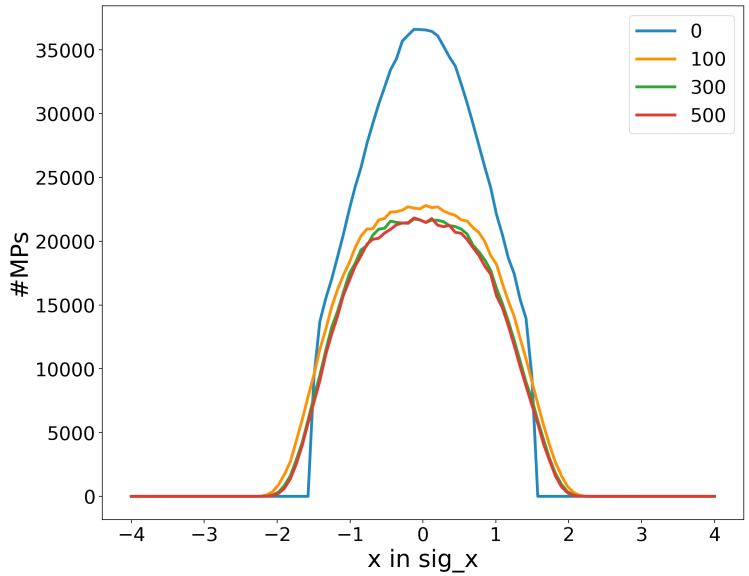

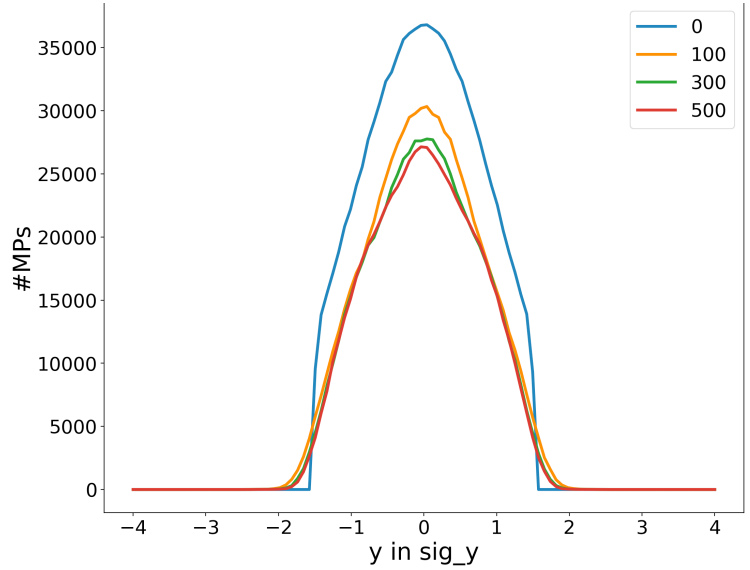

Backup - Reiser sources of emittance growth

6.1
Causes of Emittance Change

In the self-consistent theory of Chapter 5 we limited our analysis for the most part to stationary or quasistationary beams where the applied focusing forces are linear and the emittances associated with each direction are constant. These beams are best described by a Maxwell–Boltzmann distribution with different transverse and longitudinal temperatures. The forces arising from the space charge of such stationary beams are in general nonlinear except at very low temperatures, where the perveance dominates over the emittance and where the transverse density profile tends to be uniform. However, in the equilibrium state the nonlinear space-charge forces do not, by definition, cause any changes in temperature and emittance.

Real laboratory beams are usually not in perfect equilibrium, and there are a large number of effects that can cause the temperature and emittance to increase.

The most important causes of emittance growth are the following:

- Nonlinearities in the applied forces
- Chromatic aberrations
- Nonlinear forces arising from nonstationary beam density profiles
- Beam mismatch causing oscillations of the rms radius
- Beam off-centering causing coherent oscillations around the optical axis or central orbit
- Misalignments of the focusing and accelerating elements
- Collisions between the beam particles (Coulomb scattering) and between the beam and a background gas or a foil
- Instabilities, including unstable interactions with applied or beam-generated electromagnetic fields
- Nonlinear single-particle resonances and nonlinear coupling between longitudinal and transverse motion (especially important in circular accelerators)
- Beam–beam effects in the interaction regions of high-energy colliders

Taken from “Theory and Design of Charged Particle Beams”, second edition, 2008

Mechanisms of emittance growth induced by space charge forces

TABLE I.
MECHANISMS OF EMITTANCE GROWTH
INDUCED BY SPACE-CHARGE FORCES

	Charge Redistribution	RMS Mismatch	Thermal-Energy Transfer	Structure Resonance
Free-energy source	Nonuniform field energy	Potential energy	Thermal energy in other plane	Directed energy
Focusing system	Uniform and periodic	Uniform and periodic	Uniform and periodic	Periodic
Time scale	$\sim \tau_{\mathrm{plasma}}/4$	$\sim 10\tau_{\mathrm{plasma}}$	$\sim 10\tau_{\mathrm{plasma}}$	$\sim 2\tau_{\mathrm{betatron}}$
Distribution function sensitivity	Strong	Weak	Weak	Strong
Emittance growth formulas	Yes	Yes	Yes	No
For minimum growth	Uniform density or internal match	rms match	Equipartition	$\sigma_0 < \frac{\pi}{2}$

Emittance growth from space-charge forces, Thomas P. Wangler, AIP Conference Proceedings 253, 21 (1992); https:// doi.org/10.1063/1.42143